

QUEEN MARY, UNIVERSITY OF LONDON

Artificial Skin Sensitive to Pressure

MEng Final Year Project

Queen Mary, University of London

By
Inés Jiménez Palomar

Project Supervisor: Dr. James Busfield
Co-Supervisor: Vineet Jha

7th of March, 2008

I confirm that the contents of this report are entirely my own work and that nothing has been included from other sources without acknowledgement.

Inés Jiménez Palomar

ABSTRACT

The main objective of this project was to study the properties and performance of different conductive carbon filled natural rubbers; the most interesting one being the change in resistivity when strained. These changes in resistivity under strain could serve in numerous applications, as the change could be detected and measured in order to act as a sensor such as a prosthetic artificial skin sensitive to pressure. In order to achieve this, a range of fillers have been selected in order to analyze how the different structure and properties of the fillers affect the conductivity and hence be able to design a more suitable material for such application in a future. Both reversible and irreversible behaviour were observed, the reversible being the most interesting material. The behaviour was not affected by under cyclic loading. The effect of temperature and swelling were measured. Finally, a series of models consisting of filler aggregate structures and phase transition as a model were considered in order to understand the behaviours observed.

1.0 INTRODUCTION	5
2.0 LITERATURE SURVEY	5
2.1 Rubber Physics	5
2.2 Filled Rubbers	6
2.3 Conductive Rubbers	7
2.3.1 <i>Percolation - Theory and Threshold</i>	7
2.3.2 <i>Conduction Mechanism</i>	8
2.3.3 <i>Effects of Carbon Black Particles on Resistivity</i>	9
3.0 MATERIALS	10
3.1 Natural Rubber filled with Carbon Black	10
3.1.1 <i>Rubber</i>	10
3.1.2 <i>Filler</i>	11
3.2 Structure and Properties of Fillers Used	12
4.0 EXPERIMENTAL TECHNIQUES AND METHODS	13
4.1 Methods	13
4.1.1 <i>Tensile Testing</i>	13
4.1.2 <i>Tensile Testing at Room Temperature</i>	14
4.1.3 <i>Tensile Testing at High Temperatures</i>	14
4.1.4 <i>Resistivity Measurements</i>	14
4.1.5 <i>Sample Preparation for Tensile Testing of Swollen Samples</i>	15
4.1.6 <i>SEM</i>	16
4.2 Calculations	16
4.2.1 <i>Stress and Extension Ratio</i>	16
4.2.2 <i>Resistivity</i>	16
4.2.3 <i>Swelling</i>	17
5.0 RESULTS AND DISCUSSION	17
5.1 Structure and Performance	17
5.2 SEM	19
5.3 Mechanical Properties	19
5.4 Printex, Effect of Strain, Temperature and Swelling on Conductivity	21
5.4.1 <i>Effects of Strain (1st cycle and cyclic loading)</i>	21
5.4.2 <i>Effects of Temperature</i>	22
5.4.3 <i>Effect of Swelling</i>	24
5.4 HAF, Effect of Strain, Temperature and Swelling on Conductivity	26
5.4.1 <i>Effect of Strain (1st cycle and cyclic loading)</i>	26
5.4.2 <i>Effect of Temperature</i>	28
5.4.3 <i>Effect of Swelling</i>	29
5.5 MT, Effect of Strain, Temperature and Swelling on Conductivity	31
5.5.1 <i>Effect of Strain (1st cycle and cyclic loading)</i>	31
5.5.2 <i>Effect of Temperature</i>	32
5.5.3 <i>Effect of Swelling</i>	33
5.6 Proposed Model	34
6.0 FUTURE WORK	41
7.0 CONCLUSION	41
REFERENCES	

PROJECT PLAN**Table of Figures**

Figure 1	Percolation Threshold. (Sok, 1994)	7
Figure 2	Filler Content vs. Resistivity. (Strümpfer et al. 1999)	8
Figure 3	Potential Energy as a function of distance from the positive ion with and without a field. (Frenkel, 1938)	9
Figure 4	Fundamental Carbon Black Properties. (Columbian Chemicals, 2006)	12
Figure 5	SEM of Printex	19
Figure 6	SEM of HAF	19
Figure 7	SEM of MT	19
Figure 8	Stress Strain curve of natural rubber, filled with the three types of carbon black fillers, all at 10phr.	20
Figure 9	Printex at Room Temperature, 1 st and 20 th cycle.	22
Figure 10	Different Filler Loadings of Printex 6, 10, 15, 17, and 20 phr	22
Figure 11	Printex at Room Temperature and at 80°C, 1 st and 20 th cycle.	23
Figure 12	Printex Swollen in Xylene, Room Temperature, 1 st cycle.	25
Figure 13	Printex Swollen in DBA, Room Temperature, 1 st cycle.	25
Figure 14	Printex Swollen in DBA, Room Temperature, 20 th cycle.	26
Figure 15	Printex, 10 and 20 phr swollen in DBA, $V_r=0.96$, 1 st and 20 th cycle.	26
Figure 16	HAF, three different fillers at room temperature, 1 st and 20 th cycle.	27
Figure 17	CDX at Room Temperature and at 80°C, 1 st and 20 th cycle.	29
Figure 18	Raven P-5 (N220) at Room Temperature and at 80°C, 1 st and 20 th cycle.	29
Figure 19	CDX swollen in Xylene, Room Temperature, 1 st cycle.	30
Figure 20	Raven P-5(N220) swollen in Xylene, Room Temperature, 1 st cycle.	31
Figure 21	N330 swollen in DBA, Room Temperature, 1 st cycle.	31

Figure 22	Raven P-5 (N220) swollen in DBA, Room Temperature, 1 st cycle.	31
Figure 23	CDX swollen in DBA, Room Temperature, 1 st cycle.	32
Figure 24	MT at Room Temperature, and at 80°C, 1 st and 20 th cycle.	32
Figure 25	MT swollen in DBA, Room Temperature, 1 st cycle.	34
Figure 26	MT Swollen in Xylene, Room Temperature, 1 st cycle.	34
Figure 27	Proposed Model (Jha, 2008)	35
Figure 28	Stress-Strain curve of Printex at 10 phr.	37
Figure 29	Stress-Strain curve HAF at 50 phr.	37
Figure 30	Stress-Strain curve of MT at 231 phr.	37
Figure 31	Adhesion Index	37
Figure 32	Parallel and Series Conductivity Model	39
Figure 33	TEM of MT (N990) carbon Black	40
Figure 34	TEM of Printex carbon black	40
Figure 35	TEM of HAF (N339) carbon black (Li et al., 2007)	40
Figure 36	Idealized and Bound Rubber Conductivity Model	41

Tables

Table 1	Composition of Materials used. (Avon, 2007)	12
Table 2	Carbon Black Properties: particle and aggregate size. (Townson and Hallet, 2005 and SangHyun Industry, 2008)	18
Table 3	Effect of morphology on selected rubber properties (Townson and Hallet, 2005)	18
Table 4	Chord Moduli of the filled rubbers all at 10 phr.	21
Table 5	Properties of rubber and their effect in performance. (Hess et al, 1967, Townson and Hallet., 2005 and SangHyun Industry, 2008)	38

1.0 INTRODUCTION

The main objective of this project was to study the properties and performance of different conductive carbon filled natural rubbers whose most interesting property is to show a change in resistivity when strained. These changes in resistivity under strain could serve in numerous applications, as the change could be detected and measured in order to act as a sensor.

For their properties and their ability to conduct, natural rubber filled with carbon black was chosen for this particular report. The combination of these materials might not be the optimal solution for this application but they show the optimal conductivity properties under strain. A better understanding of what gives them their properties could provide the basis for a better material selection for an “Artificial Skin Sensitive to Pressure” application.

This report studied the main properties of these elastomers, observing changes in resistivity under strain in different conditions. Three main types of fillers were studied, all inside a natural rubber matrix. This gave a wide variety of results and the possibility of isolating certain properties in order to study their effect.

Studying the bulk properties and the conductive properties of these elastomers, allows the possibility of revealing what is happening at the filler-rubber interface which can help in the understanding of their conductive properties in order to design a suitable material for a prosthetic skin application.

2.0 LITERATURE SURVEY

2.1 Rubber Physics

Rubbers or elastomers are polymers with a random coil molecular arrangement, hence amorphous. Unlike other kinds of polymers, such as glassy polymers and crystalline polymers, at room temperature elastomers are soft, highly extensible and elastic. These characteristics change according to the environment. They become softer when temperature is increased and stiffer and more brittle when the temperature is decreased. Changes in temperature, the addition of solvents and changes in pressure also cause the rubber to swell and affect the properties. As any kind of polymer, elastomers are divided into thermosets and thermoplastics. Thermosets refer to the rubbers in which the polymer chain is held by chemical bonds. These rubbers swell in solvents but do not dissolve and burn at high temperature but do not melt. The chemical bonds prevent these two from happening. In the case of thermoplastic rubbers, polymer chains are held by physical bonds. These do dissolve in specific solvents and soften at high temperatures.

In order to achieve specific properties and characteristics rubbers are usually mixed or compounded with different additives. These additives include: crosslinking agents or curatives; reinforcers; anti-degradants; process aids; extenders; tackifiers; blowing agents; and colorants. Unlike thermoplastics, thermosets need crosslinking agents and/or fillers in order to perform. (Hamed, 2001) This report analyzes a specific thermoset

rubber and the impact of fillers of different sizes and structures. This will be discussed further in the sections to come. The following properties provide a better understanding of the characteristics of rubber which are relevant to the application.

One of rubbers main and defining characteristics, is its ability to be deformed to a great extent and to recover completely afterwards. This is due to the flexible and mobile structured network of polymeric chains that rubber is made of which allows it to behave in this way.

The origin of the elastic force can be described as follows. When the elastomer is stretched, the polymeric chains align and the entropy decreases as it approaches a more organized state. When the load is removed, the elastomer quickly snaps back into its original shape as it wants to achieve the higher entropy state which it was in before deformation.

Rubber was selected as a skin replacement due to another very important characteristic of rubbers, recoverable deformation. Just like rubber, skin bounces back into shape when pulled or deformed, it is considered to have rubberlike elasticity. This is due to the fact that skin contains elastin which is considered to be a bioelastomer. Elastin just like rubber, is composed of chemical copolymers with irregular repeat unit sequences, which make it amorphous. A lot of the characteristics of elastin are observed in rubbers, hence the choice. (Mark and Erman, 1988)

Another of the main characteristics of rubbers, relevant to this application, is the exhibition of hysteresis which is the “failure of a property that has been changed to return to its initial value after removal of the modifying condition.” In the case of rubbers, “the relevant property [is] the stress, and the corresponding energy losses...[the] heat build up.” (Erman and Mark, 1997) Basically, it is the energy dissipated as heat when a rubber is deformed. The difference between the areas of both, the loading and unloading, curves is accounted to hysteresis.

There are a few main factors that affect hysteresis, for example hysteresis increases with a decrease in temperature and with an increase in strain rate. Hysteresis along with heat due to friction of the polymer chains and the fillers produces a heat build up. It is important to this report as the different samples show different degrees of hysteresis, which in terms of practical value for this particular application has a negative impact as the loss of energy to heat could interfere with the temperature sensors. (Busfield, 2007)

2.2 Filled Rubbers

In order to reinforce elastomer, increase tensile strength, fillers are added to the rubber. “Particulate fillers can increase the strength of an amorphous rubber more than 10-fold.” (Hertz, 2001) Carbon Black particles and Silica are commonly used as fillers. In order for a filler to be effective it must have a large surface area, hence the particles have to be small. A large surface area allows the rubber to interact with particle effectively and reduces particle-particle spacing, altogether, increasing reinforcement. Two other factors that affect reinforcement are those of the surface chemistry and structure. Surface chemistry allows increased interaction with the rubber. Aggregates are the result of

multiple carbon particles combined; structure, refers to their relationship between shape, volume and branching.

Higher structured aggregate increases reinforcement and other important properties for this application such as conductivity which will be discussed further in the report. (Hertz, 2001)

The applications of filled rubbers are numerous as they combine the great properties of elastomers while increasing the tensile strength which allows for a broader range of applications. This report concentrates on their ability of carbon black to conduct electricity and its ability to produce a change in conductivity when strained.

2.3 Conductive Rubbers

When filled, rubbers become conductive as there is a conductive path or network formed, which connects the entire system in order to allow electricity to flow through uninterrupted. The mechanisms and the theories behind this ability are further explained in the next couple of sections.

2.3.1 Percolation - Theory and Threshold

The Percolation Theory is mainly the statistical possibility of a network formation in a random disordered system. Broadbent and Hamersley defined percolation, as to oppose the use of the term diffusion as follows: “If diffusive processes involve a random walk of a particle in a regular medium then percolation processes involve a regular motion (e.g. fluid or electrical current flow) through a random medium.” This model can be used to describe how exactly electricity is allowed to flow through rubber.

The percolation model can be “consider[ed] a square lattice where each site is occupied with probability p and empty with probability $(1-p)$... [assuming] that the occupied sites are electrical conductors and the empty sites are insulators and that the electrical current can only flow between nearest neighbours. At low conductor concentration (low p) there will be many small and isolates clusters and thus no net current can flow. At large p there will be mainly large clusters spanning the complete lattice and an electrical current can flow from one side of the lattice to the other (see Figure 1 below). Thus at a certain threshold concentration p_c is called *percolation threshold*.” (Sok, 1994) This can be seen in the following figure which shows a system that has not reached the percolation threshold on the left and one that has on the right.

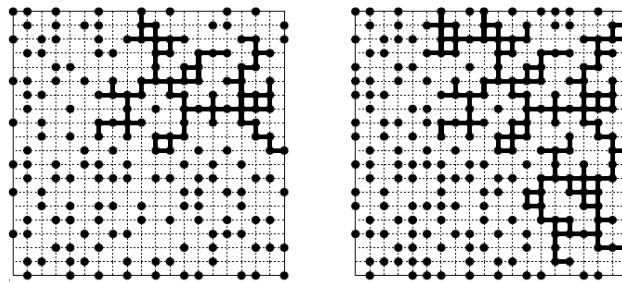


Figure 1: The system before percolation (left) and after percolation (right). (Sok, 1994)

2.3.2 Conduction Mechanisms

There are four main mechanisms that could be affecting the conductivity of the carbon filled rubber: Particle-Particle Contact related to the Percolation Threshold, Electron Assisted Hopping better known as the Pool-Frenkel mechanism, Tunnelling which is the Fowler-Nordheim mechanism, and finally Thermal Activation of the Electrons known as the Schottky-Richardson mechanism. These four mechanisms are characterized by specific trends in the plotting of different equations relating voltage and current. Relating the voltage-current data of a rubber filled system to these trends and hence mechanisms, could lead to an explanation of how the rubber is conducting electricity.

In the case of particle-particle contact, increasing the amount of particle content, increases the amount of particle contact. Once the system has reached the percolation threshold (p_c) there is a conduction path across the system, making the filled rubber conductive. The figure below (Fig.2) shows how the filler content affects the resistivity of the rubber. The higher the filler content the lower the resistivity. (Strümpfer et al., 1999)

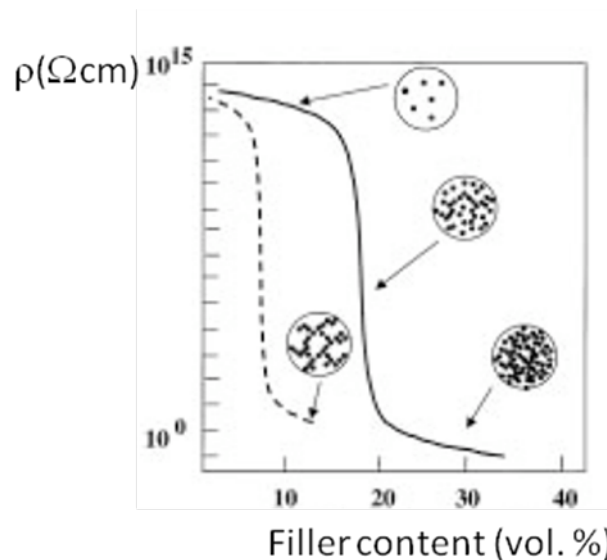


Figure 2: Increasing the filler content reduces resistivity (ρ) as a network of conductive particles is formed. (Strümpfer et al., 1999)

The Poole-Frenkel mechanism describes how in the presence of a field, the electrons are ionized and hence become free. This, causes there to be a lowering of the potential barrier. As the barrier is lowered the electrons are given the chance to “hop” and hence conduct. This effect is usually found in semi-conductors or insulators. (Frenkel, 1938)

The Poole-Frenkel mechanism is characterized by giving a positive slope, linear relationship between the $\log \sigma$ vs. $E^{1/2}$ of the following equation. (Gulalkari, R.S. et al., 2007)

$$\log \sigma = \log \sigma_0 + \frac{\beta_{PF}}{2kT} E^{1/2} \quad (\text{Equation 1})$$

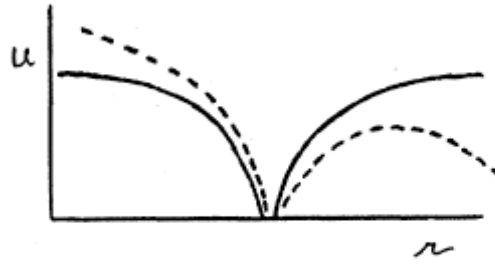


Figure 3: Potential energy as a function of distance from the positive ion. Full, line, without an external field, dotted line in the presence of the field. (Frenkel, 1938)

Tunnelling, or the Fowler-Nordheim (F-N) mechanism describes how the electrons can travel through the system freely with the help of a very large intense field, as it moves around the system instead of through. (Fowler and Nordheim, 1928)

Tunnelling is characterized by the linear negative slope of the relationship of

$\log \frac{J}{V^2}$ vs $\frac{1}{V}$ of the following equation.

$$\log \frac{J}{V^2} = \log A - \left(\frac{\phi}{V} \right) \quad (\text{Equation 2})$$

The Thermal Activation of Electrons is more widely known as the Schottky-Richardson (S-R) mechanism and it describes the effect of temperature in the conduction of electrons through the system. The thermal energy activates the electrons allowing them to move and hence produce a decrease in resistivity.

This mechanism is characterized by the relationship of $\log J$ vs. $E^{1/2}$ in the following equation.

$$\log J = \log AT^2 - \frac{\phi_s}{kT} + \beta_{SR} E^{1/2} \quad (\text{Equation 3})$$

The mechanism is temperature dependent and is helped even further when combined with the electric field effect, which reduces the potential barrier. (Gulalkari, et al, 2007)

2.3.3 Effects of Carbon Black Particles on Resistivity

There are different opinions on what is the cause of the behaviour seen in electrical conductive carbon black-polymer composites. Sau and Chaki (1998) explains that it is due to the percolation theory, the higher the loading of the filler, the higher the contact among the particles leading to the percolation threshold which in turn allows the rubber to be conductive due to the formation of the network across the system. He continues to explain that “beyond certain critical filler loading a significant drop in resistivity [is] observed. In this region a relatively small increase in filler loading produced a large increase in conductivity (decrease in resistivity). This ...rapid resistivity decrease is [due

to] the percolation region... Further increasing the filler loading beyond the percolation region causes a marginal change in the conductivity of the composite... At that time it forms a continuous conductive chain and shows stable electrical conductivity. The gradual decrease in resistivity with the increase in loading is a result of the random distribution of the aggregates in the compound.” (Sau and Chaki, 1998)

On the other hand Balberg (2001) argues that the electrical conductivity of these carbon black filled polymers is related more to the structure than to the percolation theory. He continues to argue that for many years the main explanation has always been in the area of percolation theory and inter-particle tunnelling conduction but that these two are incompatible and that “their simple combination does not provide an explanation for the diversity of the experimental results.” His argument for the incompatibility of the two concepts is based in two facts, “in contrast with the conventional percolation model, no two particles in the system are connected geometrically (as, say, in the metallic regime of granular metals), but any two conducting particles in the system are connected electrically by tunnelling.” He also raises a very good argument saying that “for different types of CBs the same volume percent of the CB phase in the composite yields very different resistivity values... [and that] both, the (apparent) percolation threshold, p_c , and the (apparent) percolation critical resistivity-exponent t depend strongly on the particular type of CB.” His approach involves the “combination of inter-particle tunnelling conduction and non-universal percolation” and he has applied it to all kinds of carbon blacks by considering the effects of the particular structures of each of the carbon blacks. The key facts are the non-universal percolation and the inter-particle tunnelling, creating a more specific model, where he explains that the tunnelling occurs only in short distances as the tunnelling conductance decays with distances and hence can only occur among neighbour particles. This then relates to the non-universal percolation model, where the particles or aggregates are not connected but the electric field flows among nearest neighbours through tunnelling. (Balberg, 2001)

3.0 MATERIALS

3.1 Natural Rubber filled with Carbon Black

This report analyses the conductive properties of natural rubber filled with five different fillers which can be categorized further into three main types, Printex, HAF and MT. In total five different filled rubbers, all with different properties. The following is a summary of the properties of both, the rubber and filler.

3.1.1 Rubber

An elastomer such as natural rubber was chosen in order to assimilate actual skin. Skin is basically an elastomer, more specifically a bioelastomer. Bioelastomers are found in different tissues such as skin, arteries, veins and in organs, such as lungs and hearts. (Mark and Erman, 1988) Natural Rubber (NR) is a hydrocarbon, a polyisoprene with the formula (C_5H_8) which builds the continuous chains. It is found naturally in a tree (Hevea

Braziliensis) in the form of a latex, in a solution which is then dried or precipitated leaving the rubber. (Treloar, 1975) In order to make it suitable for engineering applications it is vulcanized, where sulphur is added in order to combine with the isoprene chains and produce cross-linking which reinforces the system.

Natural Rubber is used in a range of applications, from building to medical. Its flexibility, resilience, high mechanical properties, extendibility and to some extent biocompatibility make this material suitable for this application. Nevertheless an issue exists, as it has the possibility of causing sensitisation due to the latex, which is an allergic reaction from long term exposure. Still, it is used in medical applications such as: membranes, diaphragms, blood pressure cuff coils, seals, covers and tubes. (Ingles, 2000)

3.1.2 Filler

Carbon black was chosen for this particular application as it shows changes in conductivity due to changes in strain, temperature and swelling which can be measured in order to act as biosensors for an artificial skin application. More interestingly, the ability of one of these fillers (Printex) to be reversible increases the possibility of a bio-sensing application as a particular strain, gives a particular change in resistivity/conductivity that can be easily measured and translated into specific information.

Carbon black is “virtually pure elemental carbon in the form of colloidal particles that are produced by incomplete combustion or thermal decomposition of gaseous or liquid hydrocarbons under controlled conditions... Its applications go from tires, rubber and plastic products, printing inks and coatings. [They are influenced and] related to properties of specific surface area, particle size and structure, conductivity and colour.” (International Carbon Black Association, 2004)

Three main types of fillers were chosen for analysis: MT, HAF and Printex. Their categorization and names are given due their manufacturing process or their properties and applications. MT stands for Medium Thermal and HAF stands for High Abrasion Furnace. Printex in the other hand is given its name to its applications as it is used mainly for printing inks to be used on paper, plastics and newspapers as indicated by its main manufacturer, Degussa. Under the category of HAF fillers, three fillers were analyzed: N330, N220 which indicate natural rubbers filled with particle sizes 30 and 20 respectively and Conductex (CDX) which is a branded filler which claims to be highly conductive.

These three main types fillers were chosen as they are representations of a range of particle size, structure and percolation threshold. Each filled rubber reaches the percolation threshold at very different volume fraction loading of fillers, meaning that the particle size and the structure affect the threshold. These filled rubbers have reached the percolation threshold and exhibit changes in resistivity with strain. They all have different filler content: Printex has 10 phr, HAF 50 phr and MT 231 phr. The composition of each filled rubber can be seen in the table below (Table 1).

Table 1: Composition of Materials Used

Ingredient /(gms)	N220	CDX7055	N330	Printex	N990
NR	100	100	100	100	100
Carbon black	50	50	50	10	231
ZINC OXIDE	5	5	5	5	5
Stearic Acid	3	3	3	2	2
MBTS	0.6	0.6	0.6		
Anti-ozone wax				1.5	1.5
6PPD				1.5	1.5
TBBS				1.5	1.5
Sulphur	2.5	2.5	2.5	1.5	1.5

(Provided by Avon, 2007)

3.2 Structure and Properties of Fillers Used

Each of the carbon black fillers, Printex, HAF and MT, has a different particle size and structure, which determines their properties and their ability to interact with the rubber.

The true unit of carbon blacks is the aggregate and not the particle, although carbon black particles makes up the aggregate, the true properties of the rubber are do the aggregate's size, shape, porosity and structure (Fig. 4). This is because the particles, even though have a distribution in size due to the manufacturing process, they all tend to form a particular shape and size aggregate. (Townson and Hallet, 2005)

As well known to all rubber manufacturers there are four main properties that give the filler its characteristics once inside the rubber: particle size, aggregate size and shape (structure), porosity, and surface activity (chemistry).

FUNDAMENTAL CARBON BLACK PROPERTIES

Fineness - Particle Size Distribution



Structure - Aggregate Size/Shape Distribution



Porosity - Pore Size Distribution



Surface Chemistry - Surface Functionality Distribution



Additional Properties
Other Constituents - Sulfur, Ash, Residue, Etc.

Figure 4: Fundamental Carbon Black Properties. (Columbian Chemicals, 2006)

Particle size is the property that provides the rubber with reinforcement, higher abrasion resistance and greater tensile strength. (Columbian Chemicals, 2006)

The structure of the aggregate, more specifically the shape and the amount of branching in the aggregate give the rubber its properties. An increase in structure increases the modulus, the hardness, the conductivity, the dispersability and the compound viscosity. As explained by Townson and Hallet (2005), Columbian Chemicals Company, who is a carbon black manufacturer, devised a classification scheme with four main types of aggregates: spheroidal, ellipsoidal, linear and branched. The least structured being the spheroidal and the most structured being the branched.

Porosity also affects the surface area, as it increases, while decreasing the density. This enables specific properties to be achieved, such as modulus and electrical conductivity, at lower carbon loadings. (Columbian Chemicals, 2006) Porosity increases “the effective black loading (porous carbon blacks are less dense), and by varying the level of interaction between the polymer system and the carbon black surface. Porous carbon blacks are primarily used in plastics for conductive applications...” (Townson and Hallet, 2005)

Surface activity and chemistry is given by the heat process in the manufacturing process, it affects the modulus, hysteresis tensile strength and abrasion resistance.

These properties will be discussed further later in the report, comparing the known properties of the fillers and the structured observed in TEM and SEM with the experimental results.

4.0 EXPERIMENTAL TECHNIQUES AND METHODS

4.1 Methods

In order to measure the changes in resistivity with changes in strain in different conditions, all five filled rubber samples were tested in uniaxial tension on tensile testing machines. Three main tensile tests were carried out: at room temperature with unswollen samples, at room temperature with swollen samples and at 80°C with unswollen samples.

All samples were cut to be rectangular shapes of a width of 24 ± 1 mm, length of 130 ± 10 mm and thickness of 2.2 ± 0.1 mm. The error in measurements of the length and area of the cross section of the sample was minimized by using the thickness gauge. The area in measuring the thickness area was 0.1%, which would mean an error of 1% length in area.

4.1.1 Tensile Testing

The tensile testing machines were operated manually, to allow the machine to be stopped at any time to measure the resistivity. The samples were loaded up to 100% strain and then down for a 1st cycle, recording force, displacement, voltage and current every 8mm, waiting 15secs after the resistivity measuring clamps were placed on the sample in order

to measure voltage and current accurately. After the first cycle, the sample was loaded and unloaded 18 more times without recording any data; the 20th cycle was then recorded. The 1st and 20th cycle can give a measurement of the difference in change of resistivity as the aggregates are re-arranging (1st cycle) and when they are already re-arranged (20th cycle).

The same pair of grips was used all throughout the experiments. In order to tightly grip the rubber sample, two identical aluminium grips were used to hold each side of the sample, each grip was tightened with two screws. Two squared pieces of rubber were placed on each side of the rubber, in order to avoid the grips causing failure at the grip and to insulate the sample from the metallic grips. The pair of aluminium grips was held by two bigger grips that connect to the tensile testing machine as per normal.

4.1.2 Tensile Testing at Room Temperature

The room temperature testing, both swollen and un-swollen, was done on a Hounsfield tensile testing machine with a load cell of either 1kN or 2.5 kN depending on availability. The first and twentieth cycle was loaded and unloaded at a speed 100mm/min while the cyclic loading in between was made at a speed of 500mm/min. The error from the load cells is considered to be negligible and hence the error in stress is 0.5%.

4.1.3 Tensile Testing at High Temperatures

The tensile testing at 80°C was done using an Instron tensile testing machine with an environmental chamber. The speed for the 1st and 20th cycle was kept to 20mm/min and was increased to 100mm/min for the cyclic loading in between. The chamber had to be opened and closed in order to insert the clamps on to the sample.

The sample was placed inside the chamber at a temperature of 80°C and closed. Once the temperature reached 80°C the sample was loaded 8mm. The chamber was then opened and the clamps were inserted at the middle of the sample and the door was closed quickly. Depending on the risk of burning the sample, the measurements were recorded within 5 to 15 seconds allowing both the resistance and the temperature to stabilize. The chamber was opened once again in order to remove the clamps. This was repeated every 8mm in both when loading and unloading the sample. Although these set of experiments were done carefully as to ensure temperature was maintained and measurements were always done at the specified temperature, there was always a drop of 1-3°C when the door was opened which although unlikely could have given a small error.

4.1.4 Resistivity Measurements

The resistivity was measured by using specially made clamps with four connections, as to achieve four point contact method in order to reduce the contact resistance effect. The specially made clamp has four copper parallel contact points that were long enough to go across the width of the sample. The two outer connections measured current (in amps) and were connected to the applied voltage (source) and the ammeter, while the two inner connections were connected to the voltmeter. The distance between the voltage points

was of 5mm. These clamps were placed across the width of the sample, always exactly in the middle and perpendicular to the sample. The applied voltage was carefully selected for each of the rubbers as to avoid burning produced by the localized increase in temperature created by the current. The more conductive the sample is, the higher the current, hence less voltage is applied as to reduce it. A balance between the risk of burning the sample and getting a measurement was always considered. The current was carefully monitored as to not reach or surpass 10mA as this current could burn the sample. The applied voltage for each of the samples was set as follows: for Printex, which was the most conductive rubber tested, the applied voltage was kept low, between 20-30V; HAF was kept from 50-80V while MT was always higher due to its low conductivity, ranging from 70-134.7V

(maximum value of the source). Since the conductivity was also affected by temperature and solvent content, the applied voltage was increased or decreased in order to balance these factors; for higher temperatures, less voltage was needed as not only does the sample become more conductive but the current increases at higher temperatures as per normal; and voltage had to be increased with increased solvent content as the samples became less conductive.

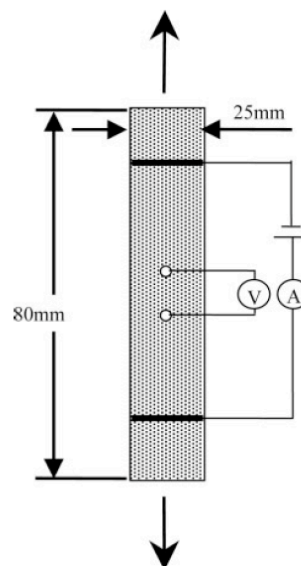


Figure 4: Schematic of method in which resistance was measured. (Busfield et al., 2005)

4.1.5 Sample Preparation for Tensile Testing of Swollen Samples

The swelling of the samples was carried out using two different solvents, DBA (dibutyladipate) and Xylene. DBA has a density of 0.962g/ml and is a more viscous and oily solvent while Xylene with a density of 0.87g/ml is less viscous and volatile. All five of the samples were swollen to different volumes inside a glass beaker which contained enough of the solvent for full submersion. The sample was left inside the solvent for specific amounts of time. The amount of solvent absorbed (the change in mass) at specific times was recorded and a mass uptake curve was calculated. The mass uptake curve was calculated for each sample in each of the solvents in order to determine the time it took to reach equilibrium as to ensure the solvent has been uniformly and fully absorbed when testing.

The samples were first weighed accurately on an electronic scale when unswollen, then submerged inside a solvent and swollen for specific times (70 secs to 210 secs) following the mass uptake curve done previously. Once swollen, making sure to remove excess solvent from the surface, they were weighed again and kept inside individual medium sized sealable plastic bags, folded around the sample as to maintain the solvent content and allow for equilibrium. In terms of solvent, Xylene was absorbed much faster than DBA and hence reached equilibrium in less time. Therefore the samples swollen in Xylene, were only left for 2 hours (7,2000 secs) before testing, while the samples swollen in DBA were left for around 24 hours (86,400 secs). Right before testing, the samples were weighed again to make sure the solvent volume in the rubber did not change.

Samples swollen in Xylene, due to its volatility, did show a great decrease in solvent content, while DBA showed little change, this change needed to be accounted for when swelling.

The swollen samples were then tested as per normal at room temperature conditions and specifications mentioned earlier.

4.1.6 SEM

The SEM images were taken by a SEM with a spot size of either 3.5 or 5, using 20 to 30kV at magnifications ranging from 25,000x to 100,000x in order to see the carbon particles and aggregates in each of the samples. The samples were prepared by creating a fracture surface by freezing them in liquid nitrogen until they became hard and brittle enough to fracture them using a pair of tweezers. Carefully, as to not compromise the fracture surface, the tip was cut using a sharp blade across, and placed, for the fracture surface to be facing upwards, on a sample holder suitable for the SEM. The sample was pasted on to the surface with silver cement. Due to the conductive nature of the sample no coating was needed and the image was able to be taken in vacuum.

4.2 Calculations

4.2.1 Stress and Extension Ratio

In order to get the stress strain curves from the tensile tests, the following calculations were carried out using force and displacement data. The stress (σ) was calculated as follows:

$$\sigma = \frac{F}{A_0} \quad (\text{Equation 4})$$

Where F is the force measured in Newtons and A_0 the cross sectional area.

The strain was measured as an extension ratio, λ . Where the strain is calculated to be a ratio of the extended length l and the initial length l_0 .

$$\lambda = \frac{l}{l_0} \quad (\text{Equation 5})$$

4.2.2 Resistivity

The main results are presented in the form of log resistivity, $\log(\rho/\Omega.m)$, and the calculations were carried out as shown below. R_e is resistance, V is voltage and I is current, these values are gathered from the testing through the special made clamps.

$$R_e = \frac{V}{I} \quad (\text{Equation 5})$$

Resistance is then inserted into the resistivity equation where ρ is resistivity, A_e is the instantaneous cross sectional area which is equal to the initial cross sectional area A_0 , divided by the extension ratio, λ . l_e is the distance between the two inner clamp connections. The resistivity values were logged in order to analyze the data more easily. All values are in amps, volts, and meters.

$$\rho = \frac{R_s A_s}{l_s} = \frac{R_s A_0}{l_s \lambda} \quad (\text{Equation 6})$$

4.2.3 Swelling

The volume fraction of rubber (V_r) for each sample was calculated from the initial mass in grams before swelling and the final mass, after swollen. The formula to calculate the V_r is the following:

$$V_r = \frac{V_{r.net}}{V_{r.net} + V_s} \quad (\text{Equation 7})$$

In order to calculate $V_{r.net}$, the volume of the rubber network and V_s the volume of the solvent in the swollen sample, the following calculations were carried out.

$$V_{r.net} = \frac{M_0 \times M_r}{\rho_{r.net}} \quad (\text{Equation 8})$$

$$V_s = \frac{M_f - M_0}{\rho_s} \quad (\text{Equation 9})$$

Where M_0 is the initial mass and M_f is the final mass after swelling, calculating the difference gives the mass uptake. M_r is the mass fraction of rubber which can be calculated by taking the ratio of the mass of the polymer and the sulphur divided by the total mass of the mix, for Natural Rubber the mass fraction is 0.94. $\rho_{r.net}$ and ρ_s are the densities of the rubber network and the solvent respectively. (Yamaguchi, 2002)

5.0 RESULTS AND DISCUSSION

5.1 Structure and Performance

This report analyzes three different types of carbon blacks, all with different properties. In order to relate how each of the properties affects the performance Table 2 shows the three different types of fillers, their particle size and their aggregate size and Table 3 shows the effect in performance of these properties.

Printex has the smallest particle size and is considered to be a branched filler which can be easily seen in the TEM image (Fig. 34, nearly at the end of the report), hence it is considered to have the highest structure of the three while MT has the largest particle size

and has a spheroidal shape as shown on TEM image and the SEM image (Fig. 33 and 7 respectively), making it the least structured. HAF, specifically N330 is considered to have branched shape and similar particle size to Printex as well but it is definitely less structured than Printex as seen in Fig. 35. Experimental data suggest that the structure plays a big role on the reversibility shown by Printex compared to N330.

Table 2: Carbon Black Properties: particle and aggregate size.

	MT	HAF			Printex
	N990	Raven P5 (N220)	N330	CDX 7055	Printex
Mean primary aggregate size (nm)	483	78	105	181	100*
Mean carbon black particle (nm)	285	24	32	42	27

(Townson and Hallet., 2005 and SangHyun Industry, 2008)

Table 3: Effect of morphology on selected rubber properties

Rubber Property	Decreasing Particle Size	Increasing Structure	Increasing Porosity
Dispersion	Decreases	Increases	
Viscosity		Increases	
Solvent Swell		Decreases	
Hardness		Increases	
Tensile Modulus		Increases	
Tensile Strength	Increases		
Resistance	Increases		
Hysteresis (Tan δ)	Increases		Increases
Storage Modulus	Increases	Increases	
Conductivity	Increases	Increases	Increases
Interesting Fact	Higher Surface Area	Increases Oil Absorption	Enables Reduced Loadings in Conductive Applications

(Referenced from: Townson and Hallet, 2005)

5.2 SEM

The following SEM pictures show Printex, HAF (N330) and MT inside the rubber. SEM cannot be used as a form of measuring particle or aggregate size accurately nor to determine structure but it helps to see and understand better what is happening once the aggregates are inside the rubber and compare them. To accurately measure particle and aggregate size and determine structure TEM is the standard used method.

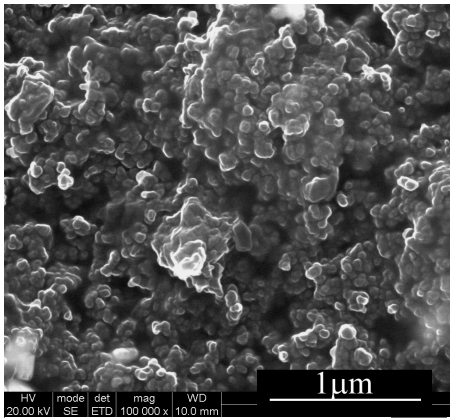


Figure 5: SEM of Printex.

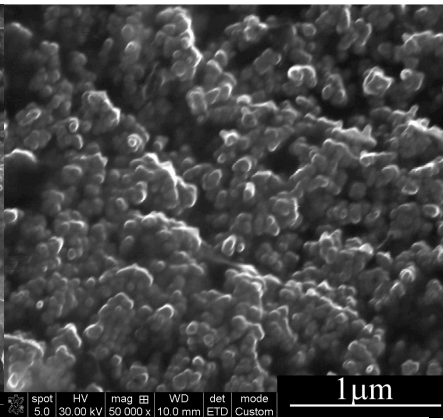


Figure 6: SEM of HAF (N330).

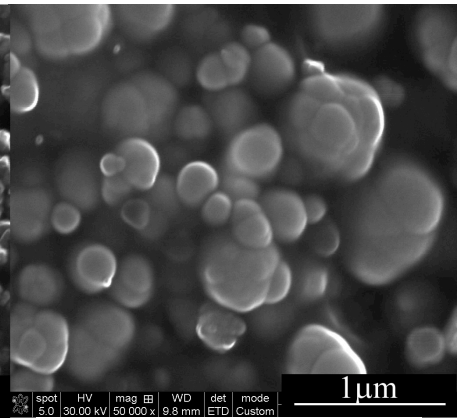


Figure 7: SEM of MT.

All three pictures have the same scale, and as can easily be corroborated, Printex and N330 have very similar particle sizes and look very similar while MT clearly has bigger particle sizes.

5.3 Mechanical Properties

In order to understand their properties further, a tensile test was conducted in order to determine their stress strain curves and hence have a better understanding of the relationship between the particle characteristics and their performance inside the rubber. Studying the performance can give clues to what is happening at the rubber-filler interface which can lead to a better understanding of the changes in resistivity observed. Fig.8 shows their stress-strain curves of all three fillers loaded at the same volume weight of 10phr. A single filler loading was chosen for all three in order to compare the particles performance in terms of the particle size and structure alone.

MT is the largest of all of the fillers analysed, it is an order of magnitude bigger than all of the other particles and it is also the less structured. The two properties make MT the weakest of all three as the low surface area and the lack of structure make MT particles easy to debond. From its stress-strain curve it can be seen that MT has the lowest stress value at 100% strain with a value of 0.8MPa.

For analyzing purposes, the stress strain behaviour of N330 is the only one shown in Fig.8. It is clear that HAF lies between both MT and Printex. N330 has much smaller

particle size and much greater structure than MT which makes it have a higher stress value of 0.9MPa. Although HAF is very similar to Printex in terms of particle size and

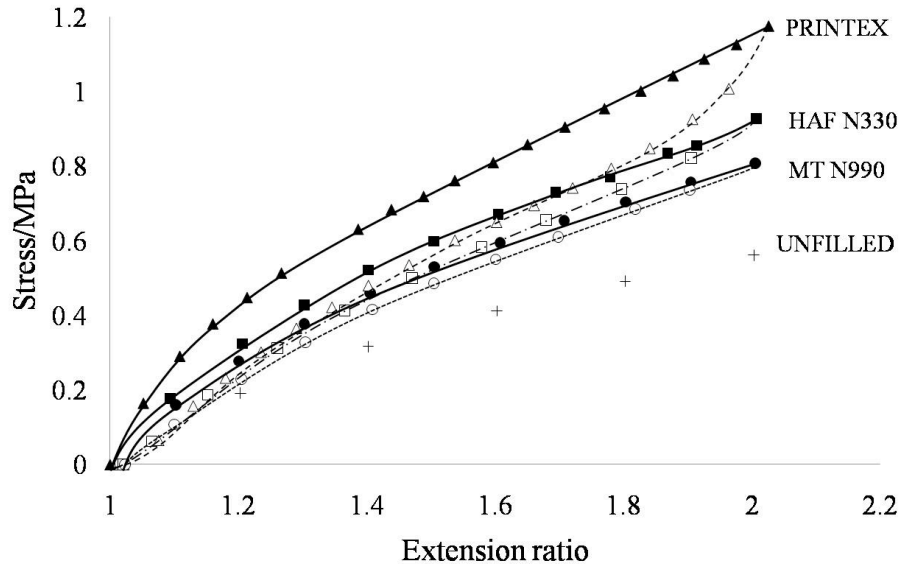


Figure 8: Stress-Strain curve of natural rubber filled with the three types of fillers all at 10 phr.

aggregate size there is probably a difference in structure and a higher porosity, which accounts for HAF having a lower stress value.

Printex has the smallest particle size and the highest structure making it the hardest to debond of all three. Therefore Printex has the highest stress value at 100% strain of all three, it being 1.2MPa.

The graph above (Fig.8) also shows the different amounts of hysteresis that occur in all three kinds of filled rubbers. This “hysteresis loss of carbon black filled rubber.... may be attributed to (1) molecular frictions accompanying deformation of the gum phase, (2) polymer-filler detachment, and (3) breakdown of filler structure and weak rubber chains.” (Kar and Bhowmick)

After the rubber has been loaded once “...the hysteresis loss decreases drastically in the second cycle and attains a plateau value at the fourth cycle. The change is insignificant after this. The loss is more at higher loading or at higher rates of testing...” (Kar and Bhowmick)

MT has the lowest hysteresis of all three at 10phr as it probably does not dissipate much energy as the particles are probably well dispersed and as mentioned in Table 3, the larger the particle size the lower the hysteresis. A higher filler loaded MT, such as the 231 phr MT used in this report, is usually used in damping applications that require energy to be absorbed quickly and effectively. The ease of debonding of the MT particles allow it to be great for this application. The stress-strain curve of MT can be seen in Fig. 30 later in the report. In this case the hysteresis is large and this is probably due to the energy release due to the amount of debonding occurring.

HAF has a smaller particle size than MT, hence there is a slight increase in hysteresis, as more energy is required to debond the particles. As can be seen in Fig.29 Raven P-5 (N220) which is the HAF filler with smallest sized particles shows more hysteresis than the other two which in turn show very similar amounts even though they both have different particle sizes.

Printex shows the biggest amount of hysteresis as it has the smallest particle size, this is also due to the probability that it has the highest porosity although there is no evidence of it as the OAN (Oil Absorption Number), which can measure structure and porosity by measuring the amount of oil that can be occluded along the structure, does not give a higher value than that of N330. The Oil Absorption Number also gives a measure of how much polymer can be occluded along the branches which produces an increase in the modulus and viscosity. (Townson and Hallet, 2005) The higher the number the more energy is required to debond the aggregates. From the experimental data, Printex should have a higher OAN as can be seen from the hysteresis observed in Fig.8 above, it does not. (These values can be compared in Table 5.)

Table 4 –Chord Moduli taken at 10% strain from stress-strain curve at 10phr (Fig.8).

	Printex	HAF (N330)	MT (N990)
Modulus / MPa	0.97	0.83	0.66

Also mentioned in Table 3, the tensile modulus increases with increasing structure, taking chord moduli from Fig.8 where all three fillers have the same loading, Printex can be considered to have the highest structure as it has the highest modulus.

5.4 Printex, the effects of Strain, Temperature and Swelling on Conductivity

5.4.1 Effects of Strain (1st cycle and cyclic loading)

Printex is the most unique of the three fillers as it shows reversibility. Figure 9 shows cycles 1 to 20 with no change in the behaviour with strain. There is a constant change in resistivity of ~2 orders of magnitude (~1.7 to 4.5Ω.m) when strained. The reversibility of Printex was already observed by Flandin et al. in 1999, but the rubber matrix was ethylene-octene and the samples were only strained to 20% which could be not enough to break the conductive network.

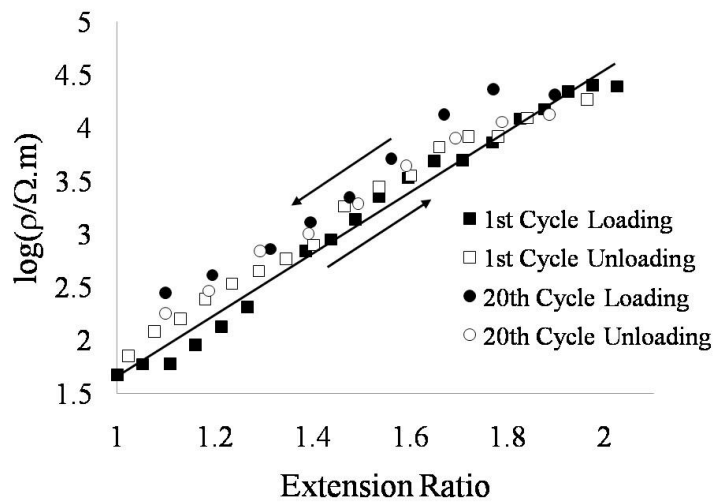


Figure 9: Printex at Room Temperature, 1st and 20th cycle.

This was further studied by testing the change in resistivity with an increase in strain at different carbon loadings of Printex. The following graph shows the different filler contents in terms of parts per hundred of rubber (phr). As the loading increases, the resistivity decreases, hence becomes more conductive. At 20 phr, when the rubber is fully percolated, the effect of conductivity becomes independent of strain as can be seen in Fig.10 where the data is almost a straight line.

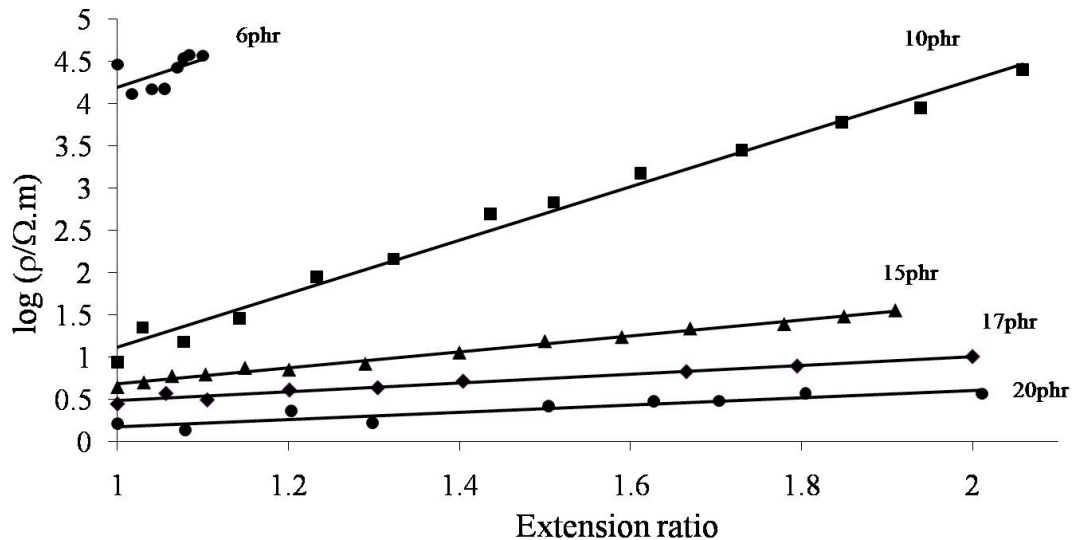


Figure 10: Different filler loadings of Printex, 6, 10, 15, 17 and 20phr.

For this application, an ideal loading would be of 10phr. As Fig.10 shows it is the loading that shows the largest change in resistivity with a change in extension. This could make it easier to measure, as there does not need to be a large change in extension in order to measure a change in resistivity.

5.4.2 Effects of Temperature

An increase in temperature produces an expansion of the rubber matrix which logically would produce an increase in resistivity as the particles move further apart, interrupting the conductive network. (Busfield et al., 2004) However experimental data shows how the opposite is true. In the graph below (Fig.11), it is clear how Printex becomes more conductive as temperature increases. The effect of temperature on conductivity in Printex has an effect of one and half to three orders of magnitude at the beginning of the loading cycle and at the end respectively (from $\sim 0.2 \Omega.m$ to $\sim 1.6 \Omega.m$ and from $\sim 2 \Omega.m$ to $4.7 \Omega.m$).

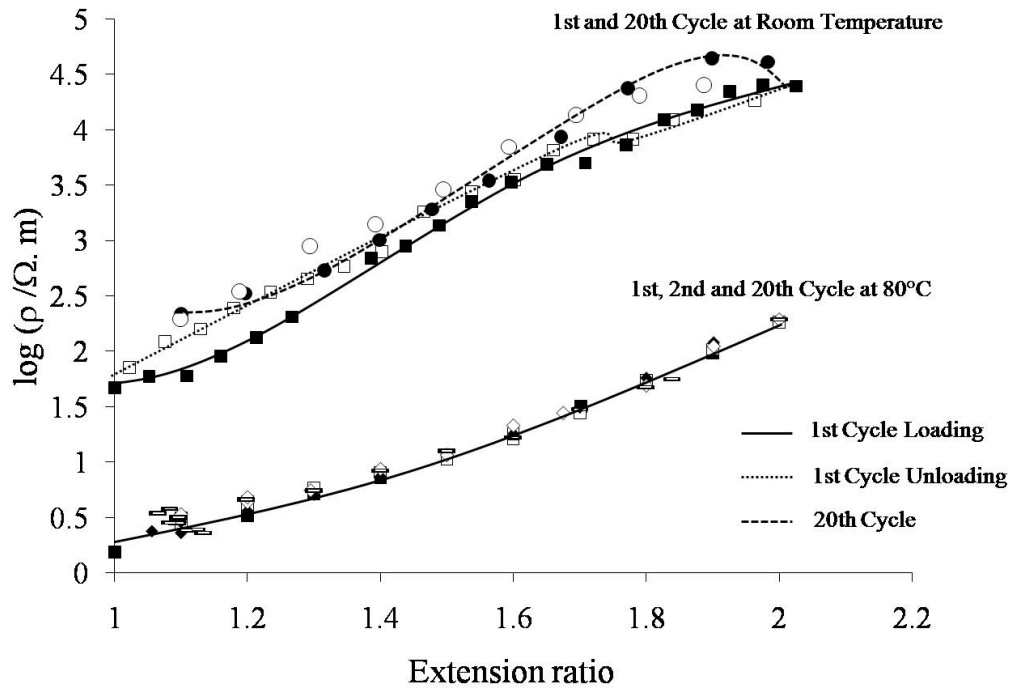


Figure 11: Printex at Room Temperature and at 80°C, 1st and 20th cycle.

This can be explained by three different effects that could be affecting conductivity. (1) Temperature adds energy to the system which in turn increases the effect of Thermal assisted hopping. (2) The particles/aggregates/polymers try to achieve the stability lost in the curing process by rearranging. When the rubber is cured aggregates are bound to the rubber in positions of higher energies as they are pressed into a shape. When the temperature increases particles tend to rearrange in order to decrease the energy state, hence become more stable. This rearrangement explains a decrease in resistivity as more conductive networks are formed. (3) Bound Rubber. It has been widely discussed that rubber has a surrounding layer extending a couple of nanometres which contains partially vulcanized or unvulcanized rubber. This rubber has a higher viscosity and lower modulus than the rest of the rubber matrix. When there is an increase of temperature and strain, its viscosity allows it to flow out, hence increasing the contact between the particles which reduces the resistivity.

Interestingly this reduction in resistivity with increase of temperature is not an isolated case, Sau et al., in 1998 observed it in NBR and EPDM. He attributes it to the effects mentioned above (1 and 2) but gives a third reason where he explains that “during heating some of the oxidative crosslinking at the surface takes place which promotes conductivity... due to the incorporation of polar carbonyl groups.” He also explains that although there is thermal expansion which interrupts the network the effect is not enough as to overcome the other three effects. Finally he observes that the effect of temperature is greater at lower loadings explaining that at higher loadings “there are already a large number of conductive networks active... the rise in temperature thermally activates the process further, [besides] at higher filler loadings... the simultaneous formation and destruction of conductive networks compensates each other, so the temperature effect is marginal. However, at lower filler loadings... the increased contribution of electron emission leads to higher conductivity. Moreover, a higher temperature leads to a the formation of some new conductive networks that were not previously contributing to the conduction of the system.”

5.4.3 Effect of Swelling

Instead of producing a large disruption to the network there is a small change in resistivity. The network is practically uninterrupted by the solvent. The following graphs (Fig.12-15) show Printex swollen in two different solvents, Xylene and DBA. Both have different densities and different volatilities as explained earlier in the experimental method, therefore they produced slightly different effects on the rubber as Xylene's volatility could be causing the solvent to be released unstrained and when straining.

In Xylene (Fig.12), this change is only of one order of magnitude (from 1.7 $\Omega\cdot m$ to 2.7 $\Omega\cdot m$) from the non swollen Printex with a $V_r=1$ to the ~20% swollen Printex, with a $V_r=0.82$. A V_r of 0.92 gave half an order of magnitude change. In this case Xylene produced half an order of magnitude change for every ~10% of solvent in the rubber. Compared to the MT and HAF, Printex is not affected as much by the solvent.

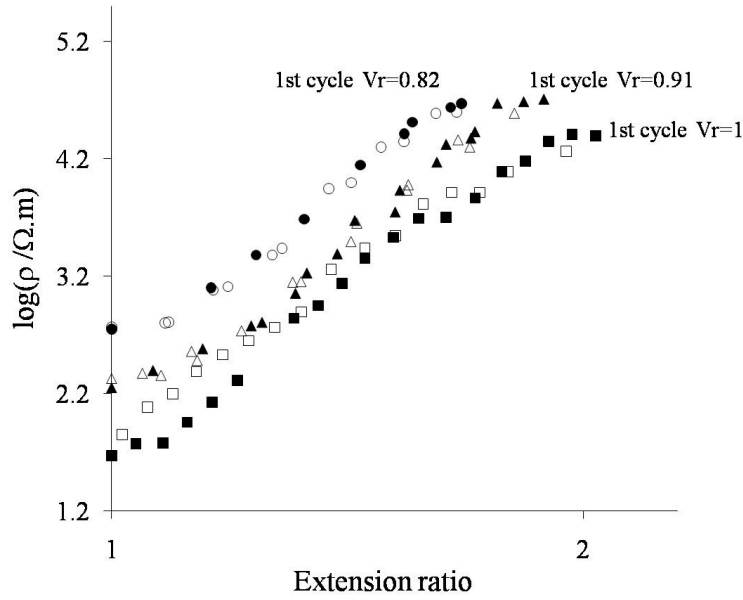


Figure 12: Printex Swollen in Xylene, Room Temperature, 1st cycle.

In DBA, it is different, as this is a much more viscous solvent. When the Printex was swollen to just ~4% ($V_r=0.96$) there was a great increase in resistivity of one and half orders of magnitude (from $1.7 \Omega.m$ to $3 \Omega.m$) but as the sample was strained resistivity did not increase as fast as in the non-swollen sample and at an extension ratio of 2, the resistivity had not reached the higher values that were recorded in the non-swollen state. A possible explanation for this is that the DBA due to its oily nature, first acted as an insulator, breaking the network of conductivity; but once the sample was strained enough, the oily solvent could have acted as a lubricant allowing the particles to move closer. This trend for this degree of swelling ($V_r=0.96$) continued even after the sample was cycled twenty times as shown in Figure 13.

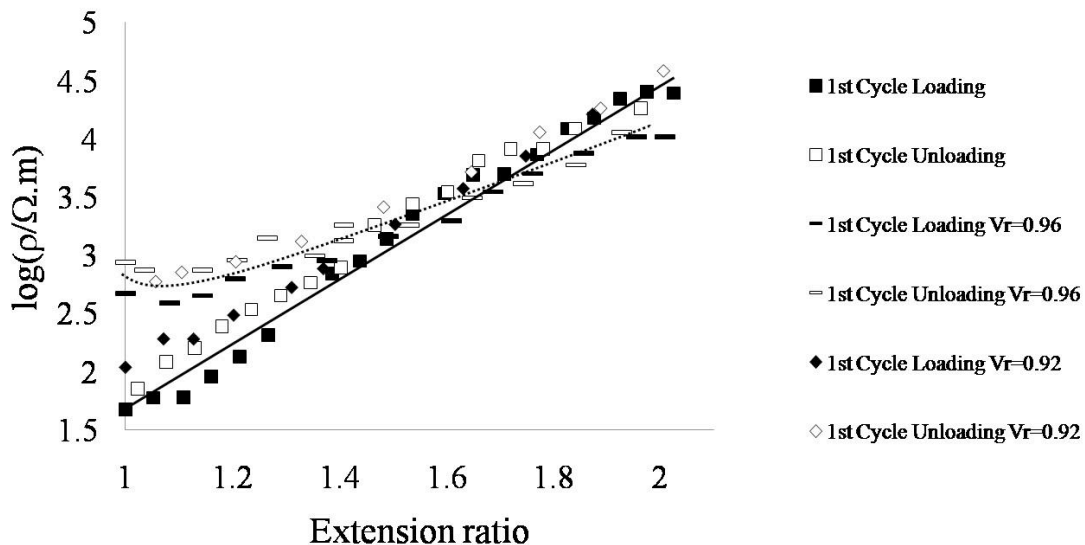


Figure 13: Printex Swollen in DBA, Room Temperature, 1st cycle.

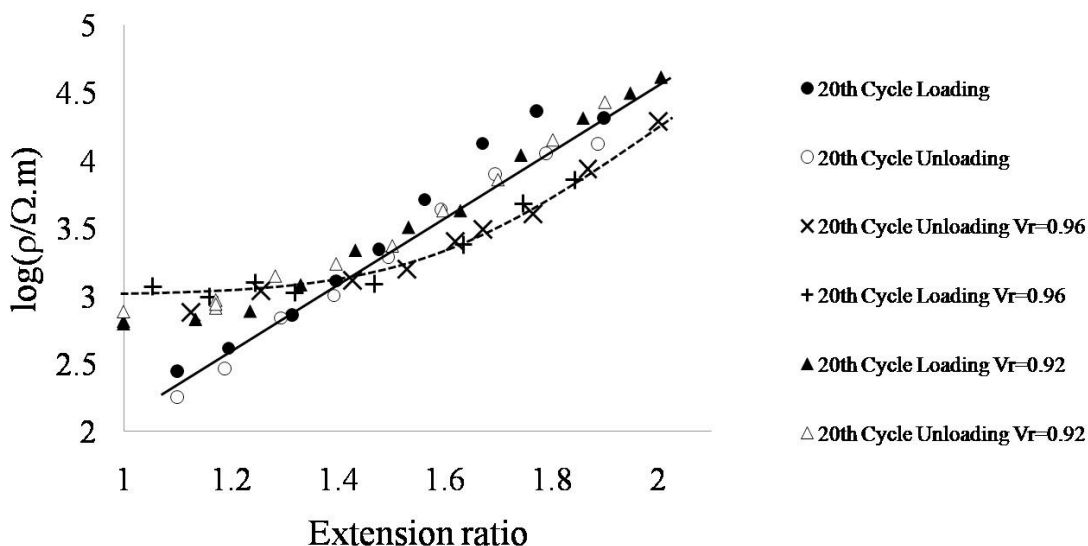


Figure 14: Printex Swollen in DBA, Room, Temperature, 20th cycle.

This is very different to what occurred when the sample was swollen to a higher degree of about ~8% in the solvent ($V_r=0.92$). When Printex was swollen even more, the initial measurement was very close to the non-swollen initial measurement and only a change of half an order of magnitude was observed. The first cycle in loading gave very similar results compared to the non-swollen and maintained the reversibility trend shown earlier. The difference arose once the sample was unloaded as can be noted in Figures 13 and 14, the unloading curve shows a similar trend given when the Printex was swollen by around 4%, giving a finishing resistivity value of 3 $\Omega.m$. This first loading-unloading cycle has within itself a change of around one order of magnitude (from ~2 $\Omega.m$ to ~3 $\Omega.m$). The 20th cycle follows the 1st unloading cycle trend which means that after the 1st cycle the Printex particles and aggregates had already rearranged completely.

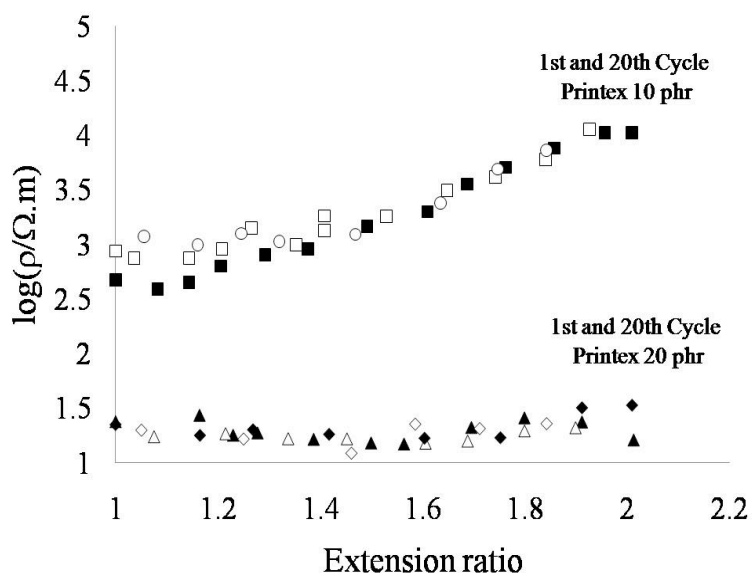


Figure 15: Printex 10 and 20phr swollen in DBA, $V_r=0.96$, 1st and 20th cycle.

In order to assess if the reversibility properties of Printex were affected in any way by the filler loading, Printex 20phr was swollen at a $V_r=0.96$ and tested (Fig. 15). Although there is a slight increase in resistivity due to the swelling, the graph clearly shows what was previously seen in Figure 10: at 20 phr, Printex shows a negligible change in resistivity with strain.

The reversibility of Printex is corroborated. Even though changes in temperature and solvent content affect the actual values of resistivity, Printex follows one similar line when loaded and unloaded, from the 1st cycle on to the 20th cycle.

5.4 HAF, effect of Strain, Temperature and Swelling on Conductivity

The effects of HAF N330 in Natural rubber have already been carefully observed by Busfield, Thomas and Yamaguchi from 2003-2005 in three papers, where they conduct strain, temperature, swelling and dynamic loading on the filled rubber. Their main observations, as mentioned earlier were the increase in resistivity with strain explained by the breakdown of the conductive network. As it reaches a maximum it starts to decrease by an order of magnitude, this is attributed to the rearrangement of the branched aggregates in N330. Upon unloading, resistivity starts to increase once more and reach even higher values than before, evidence of the extent of the damage caused by the first cycle to the network. After the first cycle, the changes in resistivity are much smaller.

5.4.1 Effect of Strain (1st cycle and cyclic loading)

The following graph shows three different HAF fillers and similar behaviours to those observed by Yamaguchi et al. 2003. Under strain, the structure breaks down. The filler then re-orientates and interacts showing the effect previously explained earlier. Therefore, when the filled rubber is strained, the particles separated and can either rearrange or stay apart giving results such as the ones seen in Fig.16 below.

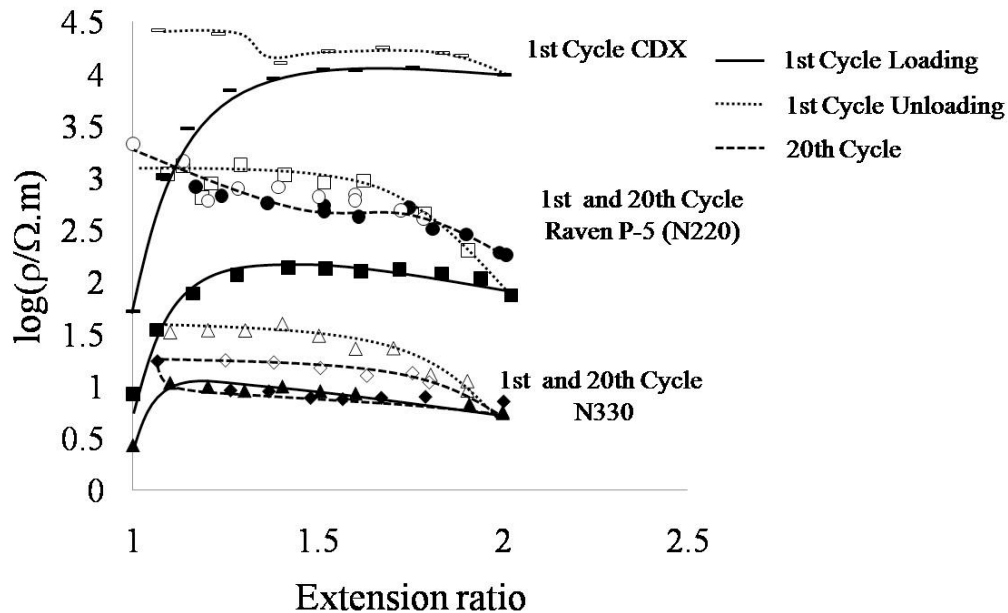


Figure 16: HAF, three different fillers at Room Temperature, 1st and 20th cycle.

The graph shows the first cycle of loading and unloading and the 20th cycle. The 20th cycle results are shown in order to portray the rubber's properties after the particles and aggregates are fully re-arranged and the network has been broken. The results for all three different types of HAF fillers: CDX, Raven P-5 (N220) and N330 can be easily compared by analysing the graph.

CDX shows a rapid increase in resistivity as it is first loaded; it increases by almost two orders of magnitudes (from $\sim 1.7 \Omega.m$ to $4 \Omega.m$). After unloaded it stabilizes and stays at around $4 \Omega.m$. This is clear evidence of particle debonding due to strain.

Raven P-5 shows similar results, showing two orders of magnitude change within the first cycle (from $\sim 1 \Omega.m$ to $3 \Omega.m$). The 20th cycle shown here further corroborates the stabilization of the rearrangement of the particles and aggregates as it similar the unloading data of the first cycle. Hence indicating that after the first cycle the particles have already fully re-arranged and further changes are negligible.

Finally, N330 was analyzed; it is shown as the most conductive of all three and the one that shows the most reversibility. As it is first loaded there is an immediate increase in resistivity of about half an order of magnitude and then it stabilizes and there is not much further change in resistivity but a slight decrease. As it is unloaded there is a change of half an order of magnitude (from $\sim 1 \Omega.m$ to $1.5 \Omega.m$). The data for the 20th cycle shows the loading curve to be the same as in the 1st cycle but again it increases slightly when unloaded. This increase of resistivity during unloading due to the following: by straining the filled rubber the aggregates debond but due to the decrease in cross sectional area there is an increase in the aggregate interactions which in turn reduces resistivity slightly. As it is unloaded the aggregates that were debonded by the loading are no longer held together by the reduction of cross sectional area and hence separate, increasing the resistivity. When the particles are loaded once again the aggregates are in close contact once more forming the conductive network which again is interrupted by unloading.

HAF is not the most suitable material of the five different ones studied in this report, as the filled rubber loses its conductivity in the first loading. In the case of N330, after the 20th cycle, there is some kind of reversibility shown but the changes in resistivity are very small and they might not be able to be detected by a sensor.

5.4.2 Effect of Temperature

The effect of temperature on HAF filled rubber is an overall reduction in resistivity, but there is no initial switching as like in Printex as the resistivity in both starts at very similar values as can be seen in both Fig. 17 and 18, CDX and Raven P-5 (N220) respectively. As shown in Fig.17, this reduction is not obvious at low very low strains but once it reaches an extension ratio of about 1.2 the effect of temperature in resistivity starts to increase giving values of half an order of magnitude lower than at room temperature. This is recurrent in both CDX and Raven P-5 (N220) and in the data gathered by Busfield et al. (2004) for N330. Once the sample reaches 100% strain the effect of temperature is different in each of the rubber samples. CDX has the lowest

change of only half an order in magnitude, Raven P-5 changes by one order in magnitude and N330 has a completely different effect as once it reaches a maximum at around an extension ratio of 1.2, the resistivity decreases until it reaches the value of the rubber tested at room temperature. Again, N330 shows partial reversibility. As already expressed in Busfield et al. (2004) temperature has very little effect in HAF filled natural rubber.

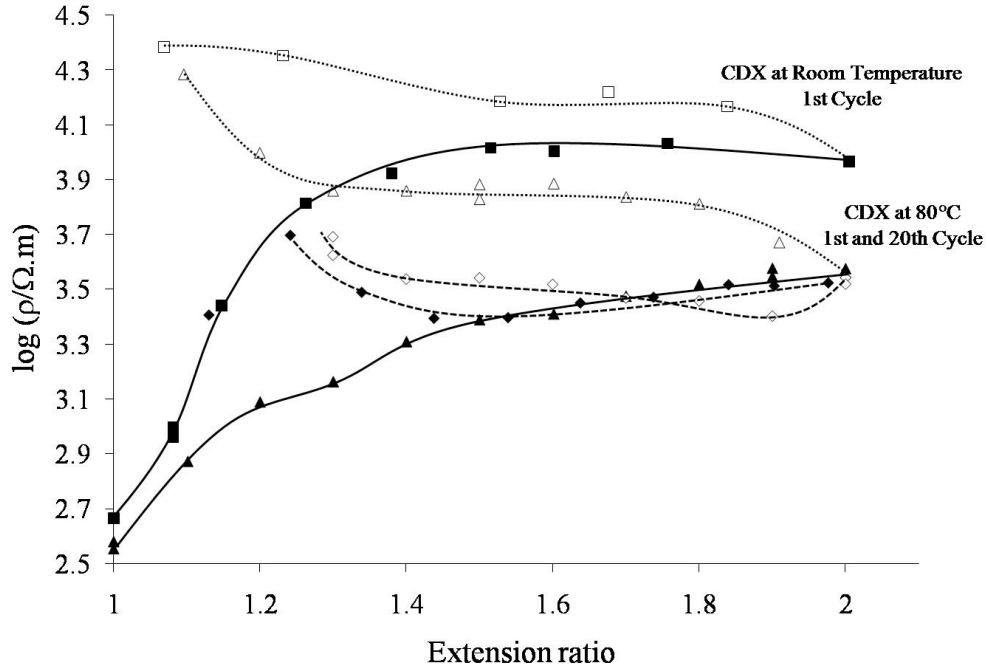


Figure 17: CDX at Room Temperature and at 80°C, 1st and 20th cycle.

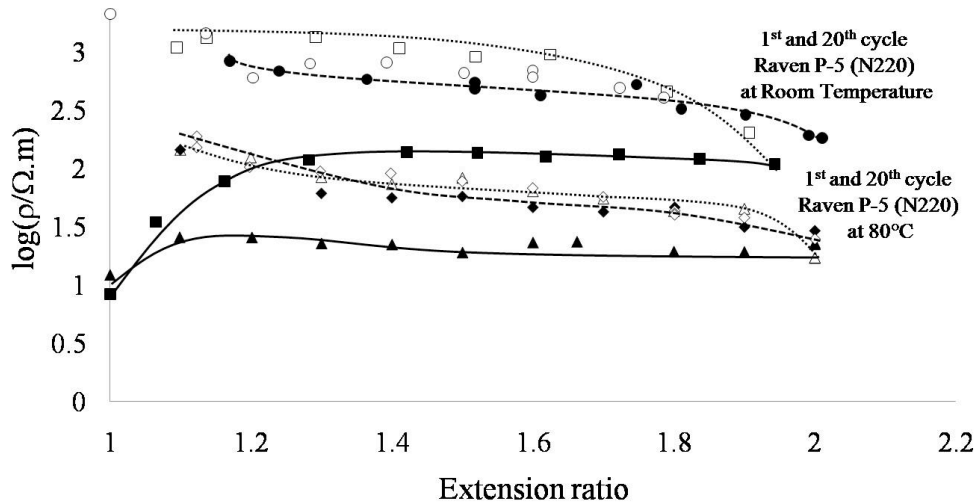


Figure 18: Raven P-5(N220) at Room Temperature and at 80°C, 1st and 20th cycle.

5.4.3 Effect of Swelling

As proposed by Busfield et al., (2004) “...swelling an elastomer in a solvent brings about a three-dimensional volumetric expansion of the rubber network. In addition, solvents

change the mechanical interaction between the rubber and the filler and they reduce the internal viscosity of the polymer matrix ... the swelling action has the effect of causing the carbon black network to break down in a manner qualitatively similar but of a greater magnitude than that caused by the application of a tensile strain. It may be that the swelling of the occluded rubber trapped in the carbon black aggregates generates substantial stresses, which can result in the aggregates being broken up. It appears that at similar strains these swelling stresses are indeed more potent than the equivalent tensile stresses in producing a breakdown of the carbon black structure.”(Busfield et al., 2004)

Once more, the filled rubber was swollen in two different solvents, Xylene and DBA. As explained earlier both solvent are very different in terms of viscosity and volatility. The following graphs represent that data gathered by swelling rubber filled with HAF carbon black at different degrees and its effect on conductivity. Figures 19 to 23 show the effect upon swelling in both solvents which has a much greater effect than the increase in temperature. In this case there is much greater effect due to Xylene than due to DBA. The results are very different for each of the types of solvent. In Xylene all three fillers have shown an increase in resistivity while in DBA, only N330 shows an increase, while both CDX and Raven P-5 (N220) show a decrease. All three samples were tested on the same day, so either there was a problem with the experiment or DBA acts differently on N330 than on the other two.

In Xylene CDX shows an initial change in resistivity of about 2.5 orders of magnitude, which is much bigger than the one observed in DBA with only an order of magnitude change. In the case of Raven P-5 (N220) there is also a much bigger change in the sample swollen in Xylene.

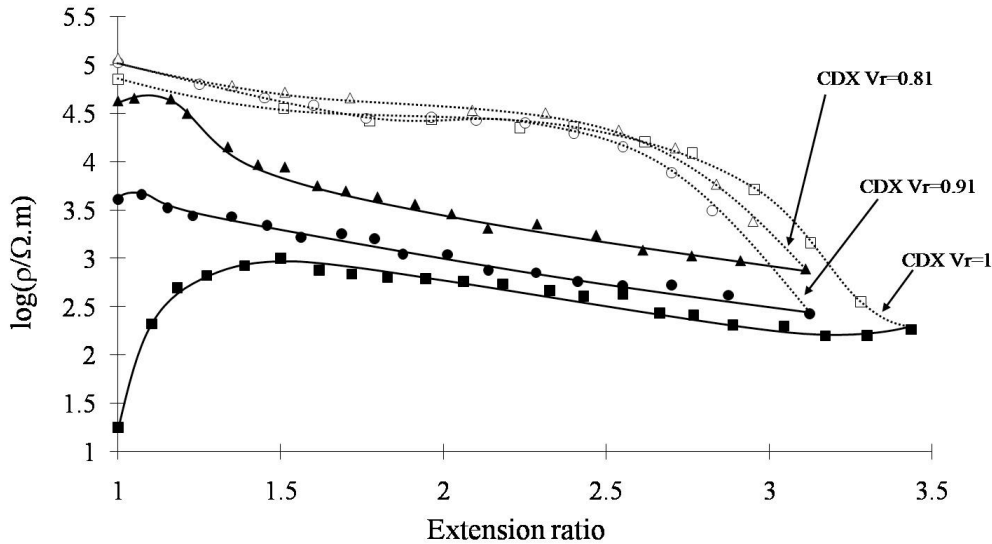


Figure 19: CDX swollen in Xylene, Room Temperature, 1st cycle.

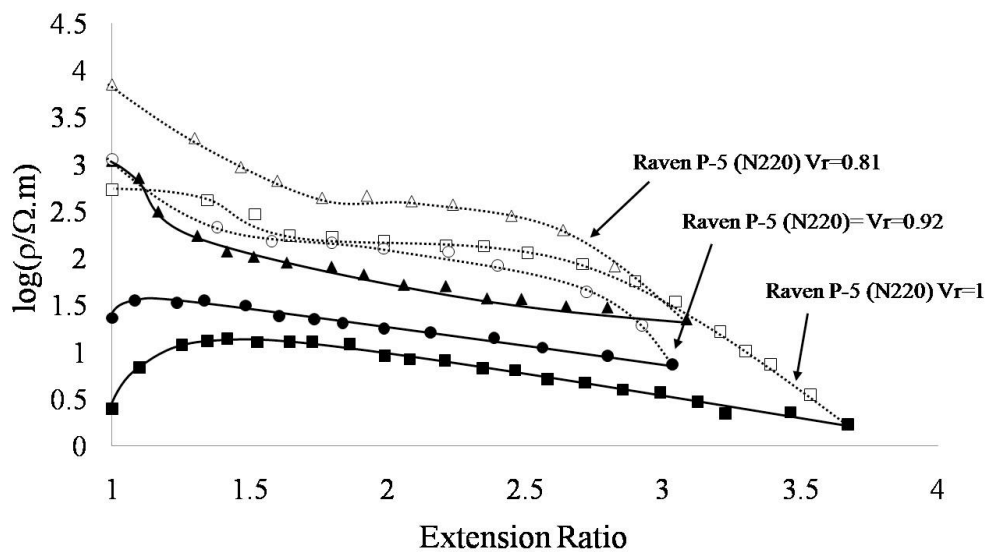


Figure 20: Raven P-5(N220) swollen in Xylene, Room Temperature, 1st cycle.

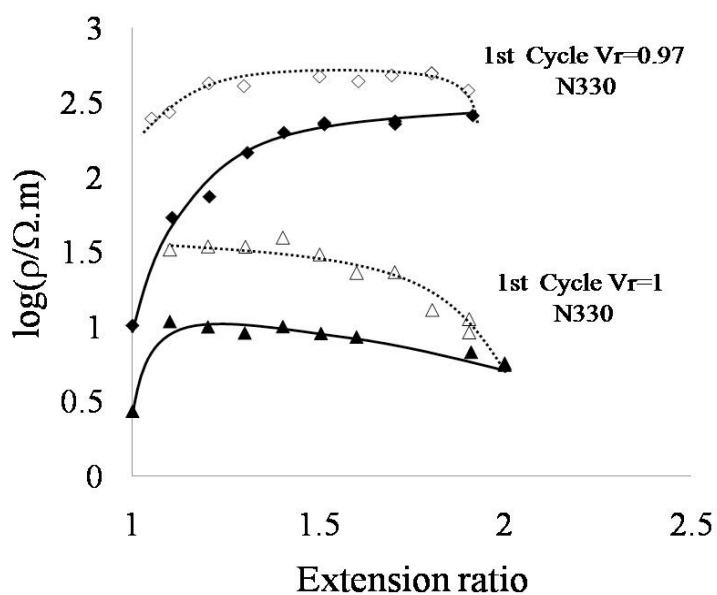


Figure 21: N330 swollen in DBA, Room Temperature, 1st cycle.

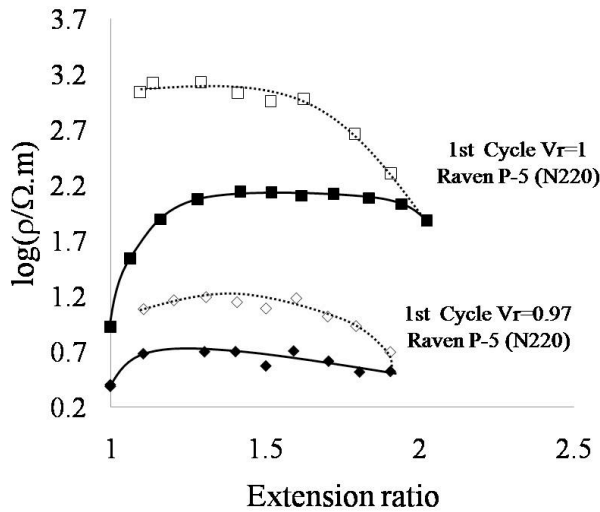


Figure 22: Raven P-5 swollen in DBA, Room Temperature, 1st cycle.

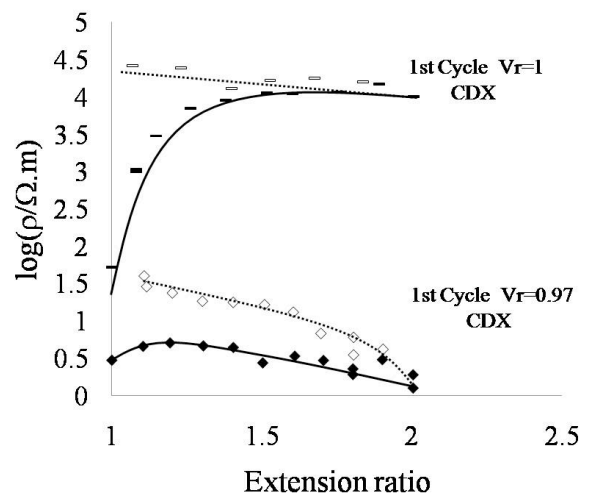


Figure 23: CDX swollen in DBA, Room Temperature, 1st cycle.

5.5 MT, effect of Strain, Temperature and Swelling on Conductivity

5.5.1 Effect of Strain (1st cycle and cyclic loading)

MT, as explained earlier, is the largest filler and the one that is the least structured, hence it has a lower surface area making the easiest to debond of all three types of fillers. When strained, the polymer and the fillers are “set free” allowing re-arrangement of the system. In this report, a highly loaded MT was used; one with 231phr, which in theory actually contains more filler than rubber. This leads to the proposal that the polymer is the one that moves around the particles rather than the particles moving around the polymer as it is more likely. This proposal might be the base for the behaviour of MT filled rubber and the effects strain, temperature and swelling has on the system.

The graph below (Fig.24) shows MT at room temperature being loaded. As it is loaded resistivity increases quickly until it reaches a peak of a change of 2.5 orders of magnitude (from about 2.5 $\Omega.m$ to 4.5 $\Omega.m$) and then starts to fall less than one order of magnitude. The unloading cycle stays at the last value of resistivity as shown in Figure 24 and increases slightly. After it is stabilized, shown as the 20th cycle, resistivity follows a similar trend as the 1st loading but inversed. As it is loaded, resistivity decreases until it reaches a minimum around the same strain as in the 1st cycle reaches a maximum and then starts to increase. This 20th cycle goes from an order of magnitude of 3.5 $\Omega.m$ down to 2.2 $\Omega.m$ and then goes back up to 3.3 $\Omega.m$. The unloading of the 20th cycle follows the loading trend but with slightly higher resistivity values.

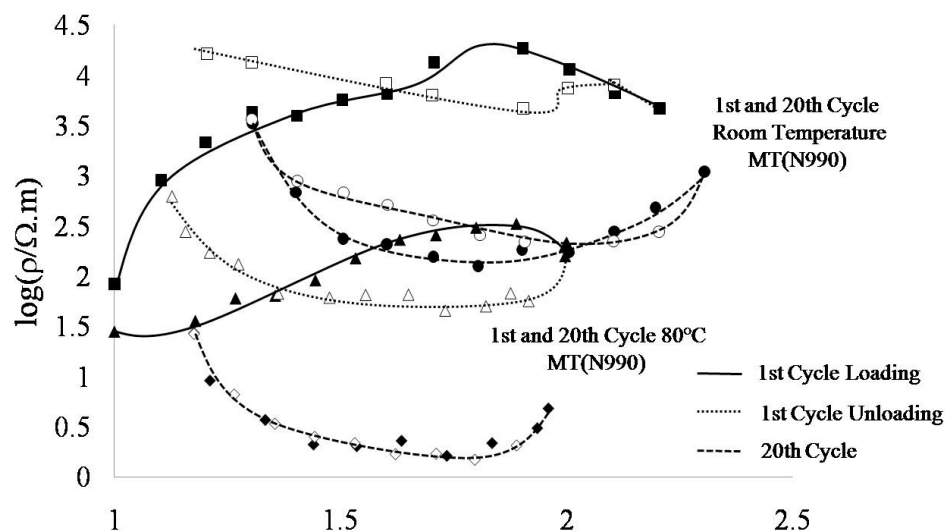


Figure 24: MT at Room Temperature, and at 80°C 1st and 20th cycle.

5.5.2 Effect of Temperature

The effect of temperature on MT (N990) is also a reduction in resistivity. Like the loading and unloading at room temperature, the 1st cycle also creates a mirrored pattern at 80° C. The cycle follows an increase in resistivity, reaching a maximum at the same point the room temperature curve reaches a maximum and then it goes slightly down as it the test was stopped at 100% strain in order to start the unloading. The change in resistivity between the maximums (at around 1.8 extension ratio) is of almost two orders of magnitude (from ~2.5 to 4.5 Ω.m). The unloading curve shows a slight increase in resistivity and a bigger one as it reaches an extension ratio of 1.2. The change in resistivity at the two minimum points of both unloading curves is also of around two orders of magnitude. The 20th cycle in this case is very similar to that of the room temperature one, but at lower resistivity values, with a change of two orders of magnitude at the beginning and end of the cycle (from ~1.5 to 3.5 Ω.m). The similar behaviour gives an indication that the aggregates react the same way to the change in strain but that there is another mechanism acting upon the system that lowers the values of resistivity, such as an increase in tunnelling due to the higher energy state.

5.5.3 Effect of Swelling

Swelling in MT filled rubber in DBA has a lower effect on resistivity than swelling it in Xylene as shown in the following two graphs (Fig. 25 and 26) The most noticeable effect in these two cases is an increase in the slope of the trend lines for both solvents. Although there is no data for a second V_r of Xylene, the highest V_r of DBA shows a further increase in slope and only a one order of magnitude change from the beginning values, but up to a change of 2.5 orders of magnitude at 100% strain.

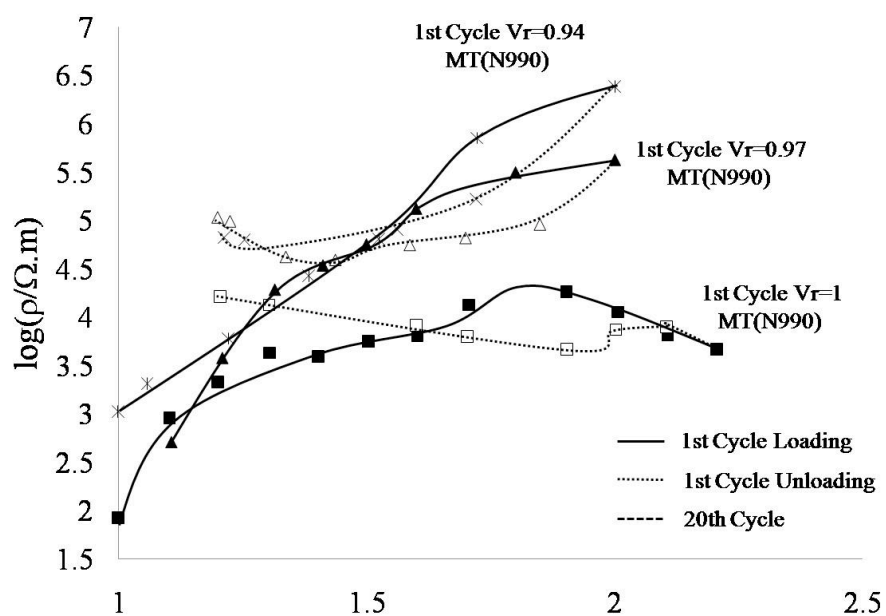


Figure 25: MT swollen in DBA, Room Temperature, 1st cycle.

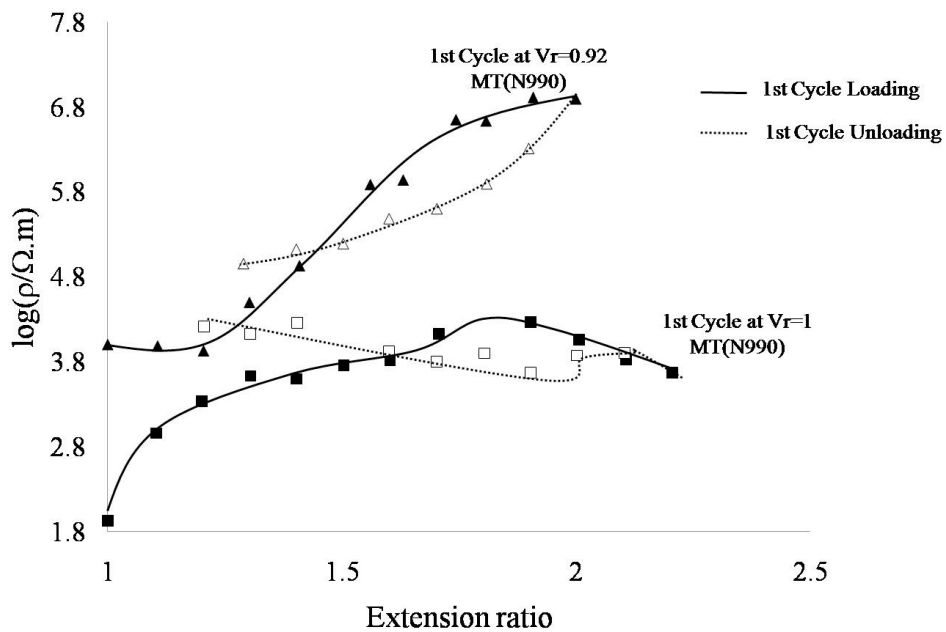


Figure 26: MT swollen in Xylene, Room Temperature, 1st cycle.

5.6 Proposed Model

In order to try to explain the effects of strain, temperature and swelling in the different types of fillers the following model is proposed. The proposed model involves five different types of aggregates. Their properties can be related back to their size and structure. In order to discuss the types of aggregates, they are going to be labelled in accordance to their performance when strained. Type 1 refers to aggregates that do not break; Type 2 to the aggregates that are reversible and go back to forming conductive networks when the strain is removed; Type 3 to the ones that are irreversible and do not reform the conductive network once strain is removed; Type 4 to the ones that do not form conductive networks in the first place; and Type 5 which are the aggregates that are debonded from the rubber, hence interrupting the rubber-filler interface.

The following figure (Fig.27) shows a schematic of each of the types of aggregates labelled at all three states, (1) virgin state, when unstrained, (2) strained state and (3) the strained state interactions, which occur due to the change in cross-sectional area due to Poisson's ratio causing different types of aggregates to interact. Type 1 aggregates do not break hence they would show no change in conductivity as they are loaded while Type 2 aggregates show a change in conductivity that is reversible, decreasing as it is loaded and increasing linearly as it is unloaded. On the other hand Type 3 aggregates show irreversible conductivity, decreasing rapidly as they are loaded but that do not go back as they are unloaded. Type 4, are aggregates that do not form a conductive network as they are not in contact with other aggregates or sufficient aggregates to form the network. Type 5 are aggregates that are debonded and have the potential to produce great changes in conductivity as the debonded polymeric

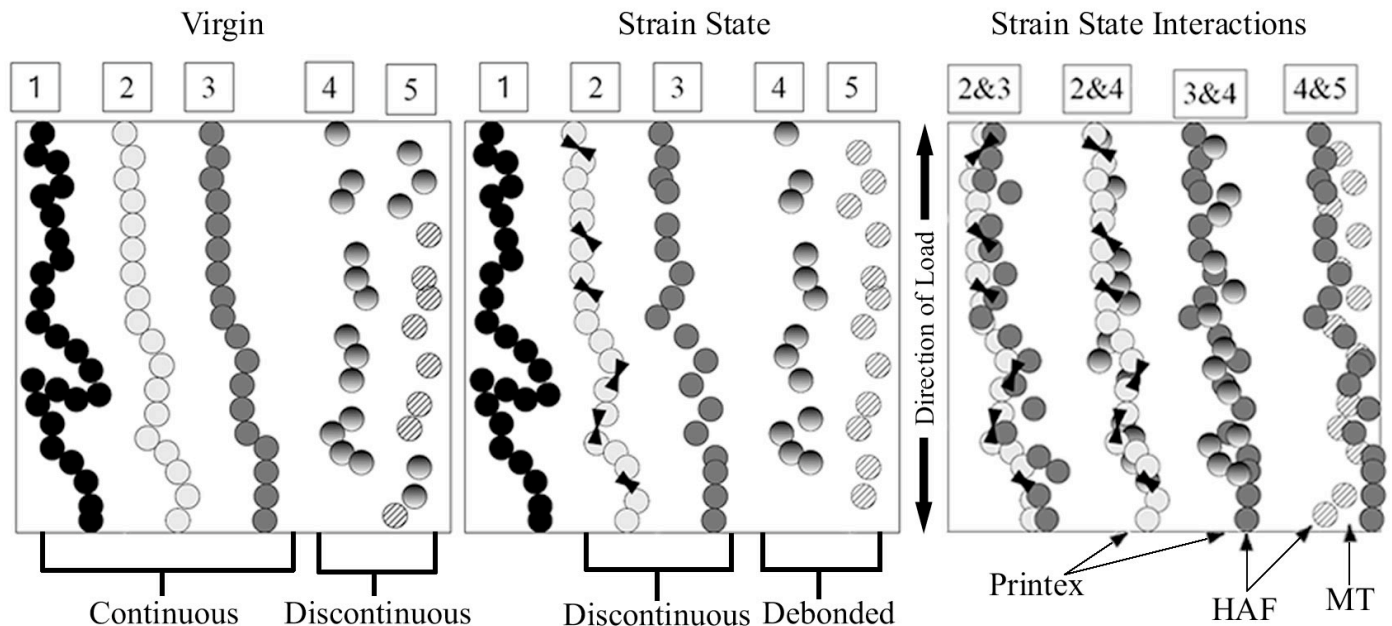


Figure 27: Proposed Model: unstrained (left), strained (middle), strain interactions (right). chains can move easily around the aggregates allowing more conductive networks to be formed, yet these also might not contribute at all.

When strained the five different types of aggregates mentioned earlier separate at different levels as specified above, potentially interrupting or re-arranging the network. Nevertheless, the strain also causes a reduction in cross sectional area which in turn causes the different types of aggregates to come in contact, producing interactions between the different types of fillers. These interactions increase the probability of the aggregates coming in contact and forming conductive networks that otherwise would not, hence increasing conductivity.

In terms of the observed effect of strain on conductivity for the different filled rubbers and the basic understanding of the properties of the fillers, the following aggregate interactions were assumed to occur. Printex is considered to have interactions of Type 2+3 and Type 3+4. HAF portrays Type 3+4 and 4+5 and MT of Type 4+5. These can further be related to the properties of each of the fillers. Printex does not debond as easily due to its structure and particle size but still shows some reversible and irreversible debonding as well as the normal isolated aggregates. The intermediate particle size and structure of HAF allows irreversible debonding to occur while the low structure and large particle size of MT means that most of the particles are not connected or debonded. Table 5, tries to gather the information in order to be analyzed further.

The type of aggregates due to their behaviours and their interactions can be further corroborated through the particle's adhesion index. The Adhesion Index is a relationship of the stress needed to see a specific percentage, at random count, of de-bonded/de-wetted particles that have surfaced. This is done using a transparent piece of rubber and placing a very thin piece of the rubber that is going to be analyzed on top, sandwiching them together and strained. A random measurement of de-wetted particles is taken. Once a specific percentage is reached, the strain is recorded. The percentage varies according to the type of fillers. (Hess et al., 1967) The adhesion index is proportional to the reinforcement. As can be seen by comparing the four graphs (Fig.28-30), as the adhesion index increases so does the reinforcement.

Figure 31 shows experimental data for MT and HAF, where a stress is recorded when the de-wetting count is of 20%. This behaviour can be explained with the proposed model. As can be seen in the graph, MT debonds at low stresses, which correlates with the Type 4 and 5 aggregates. For HAF, a bigger stress was needed in order to achieve the specific percentage. For Printex there is no data but due to the knowledge on particle structure and size and its stress strain curve, it can be estimated that the stress needed is much higher and the dewetting at 20% strain is negligible.

In order to determine the amount of dewetting at 100% strain of the filled rubbers at the filler loadings used for this report which are MT 231phr, HAF 50phr and Printex 10phr, the maximum stresses were taken from the 1st cycle stress-strain curves and compared them in order to assess how each type of filler would behave.

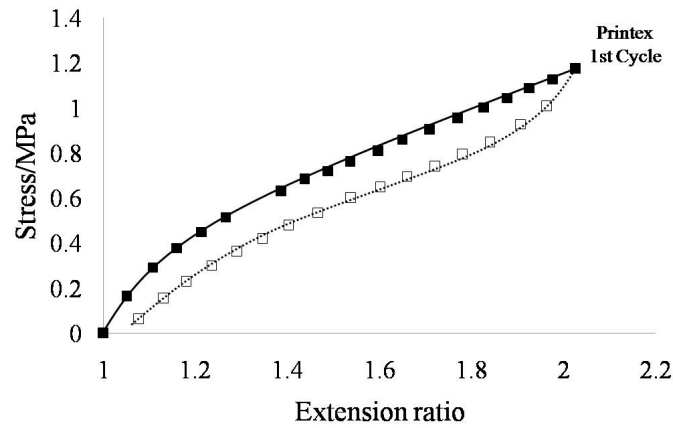


Figure 28: Stress-Strain curve of Printex 10phr.

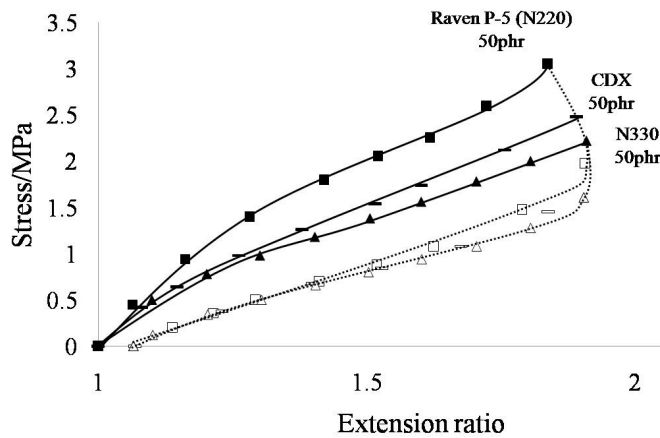


Figure 29: Stress-Strain curve of HAF 50phr.

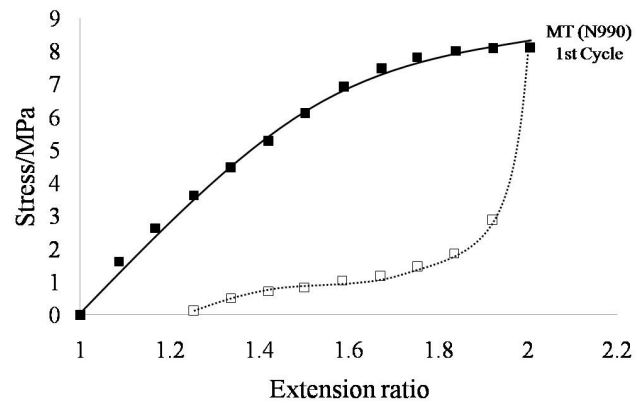


Figure 30: Stress-Strain curve of MT 231phr.

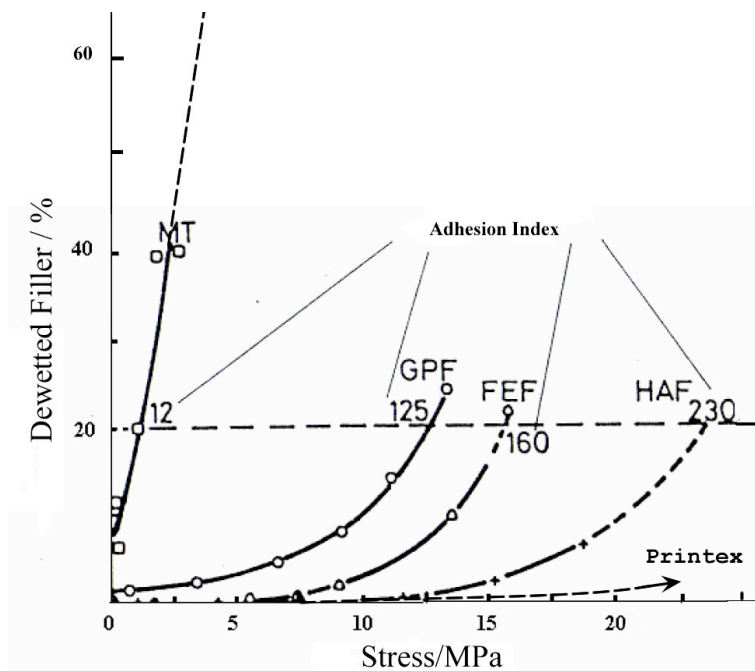


Figure 31: Adhesion Index for different filled rubbers. (Hess et al.,1967)

Table 5: Properties of rubber and their performance

	MT (N990)	HAF (N330, CDX, N220)	Printex
Volume of filler/phr	231	50	10
Particle Size	285	32, 42, 24	27
Aggregate Size	483	105, 181, 78	100
Maximum Stress at 100% strain/MPa	8	2-3	1.2
Dewetted Filler/%	>70	<2%	negligible
OAN/ml/100g (Porosity)	43	102, 122, 113	102
Surface Area	8	78, 55, 105	80

(Hess et al, Townson and Hallet., 2005 and SangHyun Industry, 2008)

The proposed model along with the adhesion indexes shows how the MT particles de-bond almost fully, aggregates in HAF have little de-bonding and that the aggregates in Printex do not de-bond. This concept leads to a model that explains the conductivity behaviour observed experimentally.

Although the proposed model explains the trends seen in each of the filled rubbers under strain it still does not fully explain why exactly occurs in terms of the resistivity/conductivity values observed and the effect of swelling and temperature. These can be better explained by the next model.

The following model represents the relationship between the highly conductive carbon filler and the insulating rubber and how an average of both could approximate the properties found in conductive filled rubbers. The graph below (Fig.32), represent the model. The line above represents the conductivity of the filler; the line below represents the conductivity of rubber and the line in the middle is a representation of the combination of both. This model involves two main forms, and their conductivity values, the Parallel and Series.

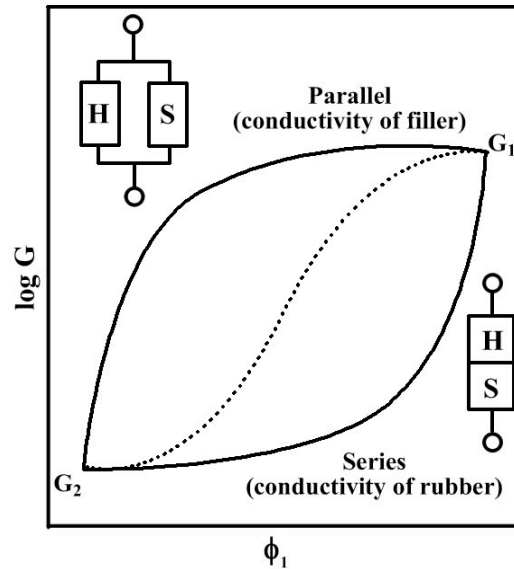


Figure 32: Parallel and Series Conductivity Model

The parallel model relates to the conductivity of the filler. This Parallel model refers to the continuous network of aggregates and depicts the idealized picture of carbon black particles touching in a straight line, like a highly conductive solid rod with a conductivity value of 670 ohms.

The series model is closely related to the conductivity of the rubber, and it depicts the discontinuous carbon black particles well dispersed in the matrix which do not form a line of conductive aggregates. The conductivity of the rubber is about 10×10^{-12} ohms.

The line that lies in the middle is a representation of an average of both which can be related closely to the values recorded for conductive filled rubbers. Printex is considered to be closer to the Parallel model while MT is considered to be closer to the Series model. The following pictures show the two extremes, Printex and MT. The two figures below, Fig.33, Fig. 34 and Fig.35, show all three: MT, Printex and HAF (N330) in TEM. Printex clearly shows the continuous chains that the Parallel model describes while MT shows the discontinuous network of the Series model.

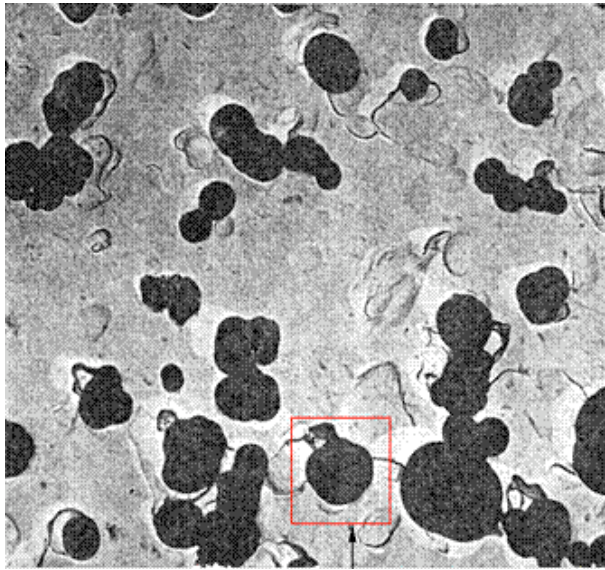


Figure 33: TEM of MT (N990) carbon black
(Source)



Figure 34: TEM of Printex carbon black
(Source)

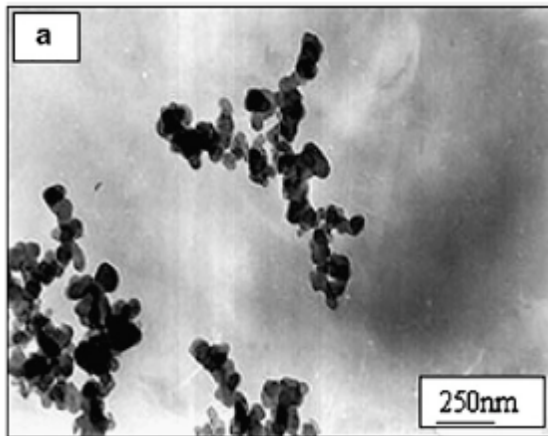


Figure 35: TEM of N330 carbon black (Li et al., 2007)

Still, the Parallel model does not fully explain the filled rubber behaviour and that is because the idea of carbon black particles in a continuous parallel network is an extreme idealization. The C-C series model is based on the conductivity of a solid carbon rod (Fig.36). A more realistic representation is that of carbon particles surrounded by bound rubber layers. This layer is proposed to be a few nanometer layer of partially vulcanized or un-vulcanized rubber which acts like a partial insulating layer, hence reducing the measured conductivity of the system. This bound rubber model gives a better approximation to the conductivity seen in the filled rubbers studied.

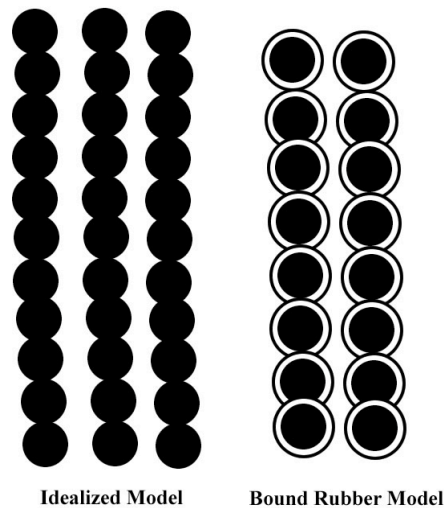


Figure 36: Idealized and Bound Rubber Conductivity Model

The bound rubber model or interface model is better explained by Fukahori who explains that the carbon blacks disperse not as particles but as aggregates and that the particles are surrounded by what he refers as carbon gel, better known as bound rubber. He explains that this bound rubber is produced during the mixing process and that it consists of two main layers: one at a glassy state, that is constrained and the unfilled rubber vulcanizate layer, a second layer which is less constrained. He also proposes a new interface model naming the two layers, the inner polymer layer which is at a glassy state he names, Glassy Hard or GH layer and outer layer which is less constrained the Sticky Hard or SH layer. He continues to explain that “due to the great activity of the surface of [the] carbon particle, several parts in a molecular chain seem to be strongly adhered to the surface of the particle in the GH layer, whether physically or chemically. On the other hand, the fact that the SH layer is also insoluble in good solvents means that a part or several part of a molecule within the SH layer is also firmly connected to the surface of the carbon particle through the GH layer... tightly entangles with the molecules extended from the GH layer.”

He also talks about the thickness of each of the layers giving the GH layer a value of 2nm and the SH layer 3 to 8nm, giving a total thickness of around 5 to 10nm. This thickness has also been mentioned in studies done by Ikeda et al., (2007) with 3D TEM imaging giving a value of 3nm thickness of bound rubber. The explanation for the difference in performance of different fillers is that “the thickness of the SH layer is smaller in the fine carbon-filled rubber than in the coarse carbon filled rubber.” (Fukahori, 2007)

6.0 FUTURE WORK

The report tries to present a model that partially or fully explains the experimental data observed although out the report. In order to determine what is the exact cause of the great reversibility shown in Printex more work needs to be carried out. A full scan of the particles has to be done, within and outside the rubber matrix. The following would serve as a start in order to comprehend its performance. Imaging methods such as 3D-TEM scans which are effectively CT Scans could help see the exact structure of each. Apart from still images, images under loading could be observed in order to be able to see the actual mechanism that allows Printex to be reversible.

In terms of bound rubber experimentation, there are extra tests that can be conducted which would consist of preparing samples of the same composition of the bound rubber and test the conductivity in order to determine if it is possible for an electric current to go through and if the values correspond to the ones observed in the carbon black filled rubbers.

In terms of developing an prosthetic artificial skin which is sensitive to touch, once the mechanisms are identified or partially identified then research should be conducted in order to find a more suitable material, which has the reversibility and switching ability of Printex; which is also biocompatible, will not swell to a great extent and that does not have the risk of causing sensitization.

7.0 CONCLUSION

After measuring the changes of resistivity of a range of fillers under different temperatures and swelling and comparing them to the room temperature one.

It was realized that:

- Fillers with low surface area and structure such as MT carbon black show irreversible behaviour; this can be attributed to the fact that they are non reinforcing fillers and debond easily, which result in the formation of a discontinuous aggregate structure.
- Fillers with high surface area such as Printex show a more reversible behaviour under all conditions. This must be investigated and analyzed using the model presented. In the present case it can be attributed to the high surface area of Printex and the hypothesis that it forms a continuous network, as is the case in the parallel network discussed.
- It was proposed in the present work that the reversible behaviour of fillers with high surface area such as Printex could be explained using the parallel model, where the fillers form continuous networks.

REFERENCES

BALBERG, I. A comprehensive picture of the electrical phenomena in carbon black-polymer composites. *Carbon*. (2002) **40**, 139-143.

BROADBENT, S.R. and HAMMERSLEY, J.M. Percolation processes. I. Crystals and mazes, *Proc. Cambridge Philos. Soc.* (1957), **53**, 629-641.

BUSFIELD, J.J.C. Notes-Rubber Materials. Dep of Materials, Queen Mary, University of London. Chp. 4, Pg. 3

BUSFIELD, J. J. C., THOMAS, A. G., YAMAGUCHI, K. Electrical and Mechanical Behavior of Filled Rubber III. Dynamic Loading and the Rate of Recovery. *Journal of Polymer Science: Part B: Polymer Physics*. (2005), **43**, 1649–1661.

BUSFIELD, J. J. C., THOMAS, A. G. and YAMAGUCHI, K. Electrical and Mechanical Behavior of Filled Elastomers 2: The Effect of Swelling and Temperature *Journal of Polymer Science: Part B: Polymer Physics*. (2004), **42**, 2161–2167.

Columbian Chemicals. “Conductex 7055 Ultra”
<http://www.columbianchemicals.com/Portals/0/Products/Literature/English/Conductex7055Ultra.pdf>, 2006. Visited on:24/02/08.

Columbian Chemicals “Raven Blacks” http://www.fitzchem.com/pdf/Raven_Blacks.pdf, 2006. Visited on:24/02/08.

Columbian Chemicals “Rubber Blacks”
http://www.fitzchem.com/pdf/Rubber_Blacks.pdf, 2006. Visited on:24/02/08.

ERMAN, B. and MARK, J.E. Structures and Properties of Rubberlike Networks. Oxford University Press, United States of America, 1997.

FLANDIN, I.; CHANG, A.; NAZARENKO, S.; HILTNER, A.; BAER, E. Effect of Strain on the Properties of an Ethylene-Octene Elastomer with Conductive Carbon Fillers. *Journal of Applied Polymer Science*. (2000), **76**, 895-905.

FOWLER, R.H, F.R.S. and NORDHEIM, L. Dr. Electron Emission in Intense Electric Fields. *Proceedings of the Royal Society of London. Series A, Containing Papers of a Mathematical and Physical Character*. (1928) **119**, 781, 173-181.

FRENKEL, J. On Pre-Breakdown Phenomena in Insulators and Electronic Semiconductor *Physical Review*, (1938) **54**, 8, 647-648.

FUKAHORI, Y. Generalized Concept of the Reinforcement of Elastomers. Part 1: Carbon Black Reinforcement of Rubbers. Rubber Division of the American Chemical Society, Inc. (2007), **80**, 4.

GALESKI, A. Strength and toughness of crystalline polymer systems. *Progress in Polymer Science*. (2003), **28**, 12, 1643-1699.

GULALKARI, R.S.; BAKALE, Y.G.; BURGHATE, D.K. and DEOGAONKAR, V.S. Electrical conduction mechanism of polyvinyl chloride (PVC)–polymethyl methacrylate (PMMA) blend film. *Pramana – J. Phys.*, (2007), **69**, 3, 485–4903.

HAMED, G.R. Materials and Compounds. In: GENT, A.N. ed *Engineering with Rubber- How to Design Rubber Components*. Munich, Hanser, 2001, pp. 11-34.

HERTZ, D. Jr. Introduction. In GENT, A.N. ed *Engineering with Rubber- How to Design Rubber Components*. Munich, Hanser, 2001, pp. 1-9.

Ikeda Y, Kato A, Shimanuki J, Kohjiya S, Tosaka M, Poompradub S, Toki S, Hsiao B S, Nano-Structural Elucidation In Carbon Black Loaded NR Vulcanizate By 3D-TEM And In Situ WAXD Measurements *Rubber Chem. Technol.* (2007), **80**, 251-264.

INGLES, D. Natural Rubber for Medical Devices. Information Center for Natural Rubber. Natuurrubber 17, 1st quarter, 2000. <http://www.rubber-stichting.info/art8nr17.html> visited on: 28/02/2008.

International Carbon Black Association. Carbon Black User's Guide – Safety, Health and Environmental Information, 2004. http://www.carbon-black.org/user_guide.html visited on: 24/02/08.

KAMAL K. KAR, ANIL K. BHOWMICK. High-Strain Hysteresis of Rubber Vulcanizates over a Range of Compositions, Rates, and Temperatures. *Journal of Applied Polymer Science*. (1997), **65**, 1429-1439.

LI, QUIYING; ZHANG, XILIANG; WU, GUOZHANG; XU, SHIAI; WU, CHIFEI. Sonochemical Preparation of carbón nanosheet from carbon black. *Ultrasonics Sonochemistry*. (2007), **14**, 2, 225-228.

MARK, J.E. and ERMAN, B. *Rubberlike Elasticity a Molecular Primer*. New York, Chichester, Brisbane, Toronto and Singapore: John Wiley and Sons, Inc., 1988.

NEAGU, E.R.; Neagu, R.M. Analysis of electric conduction mechanisms in polyethylene terephthalate. *Materials Letters*. (1998), **34**, 364-371.

SangHyun Industry, Korea. <http://www.shind.co.kr/index.php?code=0222> visited on: 4/03/08.

SAU, K.P. ; CHAKI, T.K. Electrical and Mechanical Properties of Conducting Carbon Black Filled Composites Based on Rubber and Rubber Blends. *Journal of Applied Polymer Science*. (1998), **71**, 6, 887-895.

SOK, R.M. *Permeation of small molecules across a polymer membrane: a computer simulation study*. University of Groningen, 1994.

STRÜMLER, R. and GLATZ-REICHENBACH, J. Conducting Polymer Composites. *Journal of Electroceramics* (1999) **3**, 4, 329-346.

TOWNSON, G. and HALLET, J. An introduction to the terminology used in the carbon black industry. In: AUSTRELL and KARL ed. *Constitutive Models for Rubber IV*. London, Taylor and Francis Group, 2005.

TRELOAR, L.R.G. *The Physics of Rubber Elasticity*. Great Britain, Oxford University Press, 2005.

YAMAGUCHI, K., BUSFIELD, J. J. C., THOMAS, A. G. Electrical and Mechanical Behavior of Filled Elastomers. I. The Effect of Strain *Journal of Polymer Science: Part B: Polymer Physics* (2003), **41**, 2079–2089.

PROJECT PLAN

